SYNTHESIS, CHARACTERIZATION, AND THERMAL DEGRADATION OF POLY(L-LACTIDE)S

A THESIS

SUBMITTED TO THE DEPARTMENT OF CHEMISTRY

AND THE INSTITUTE OF ENGINEERING AND SCIENCES

OF BILKENT UNIVERSITY

IN PARTIAL FULFILLMENT OF THE REQUIREMENTS

FOR THE DEGREE OF

MASTER OF SCIENCE

By

İlknur Tunç

June 2004

I certify that I have read this thesis and that in my opinion it is fully adequate, in scope and in quality, as a thesis for the degree of Master of Science.

Asst. Prof. Dr. Soner Kılıç (Supervisor)

I certify that I have read this thesis and that in my opinion it is fully adequate, in scope and in quality, as a thesis for the degree of Master of Science.

Prof. Dr. Vasıf Hasırcı

I certify that I have read this thesis and that in my opinion it is fully adequate, in scope and in quality, as a thesis for the degree of Master of Science.

Prof. Dr. Atilla Aydınlı

I certify that I have read this thesis and that in my opinion it is fully adequate, in scope and in quality, as a thesis for the degree of Master of Science.

Assoc. Prof. Dr. Ömer Dağ

I certify that I have read this thesis and that in my opinion it is fully adequate, in scope and in quality, as a thesis for the degree of Master of Science.

Asst. Prof. Dr. Dönüş Tuncel

Approved for the Institute of Engineering and Sciences:

Prof. Dr. Mehmet Baray
Director of Institute of Engineering and Sciences

ABSTRACT

SYNTHESIS, CHARACTERIZATION, AND THERMAL DEGRADATION OF POLY(L-LACTIDE)S

İLKNUR TUNÇ

M. S. in Chemistry

Supervisor: Asst. Prof. Dr. SONER KILIÇ

June 2004

In this project, 1, 2, 3, and 4-armed poly(L-lactide)s (PLs) were synthesized by ring opening polymerization (ROP) of L-lactide in the presence of an alcohol and stannous dioctoate. The resultant polymers were characterized by Gel Permeation Chromatography (GPC) and Nuclear Magnetic Resonance spectroscopy (NMR). The dynamic thermal degradation of these polymers was studied by Thermogravimetric Analyzer (TGA). In order to study the effect of end-groups on thermal degradation, the synthesized OH functional polymers were reacted with succinic anhydride to obtain COOH functional polymers. It was found that the thermal degradation temperatures of acid functional polymers are 25oC higher than those of OH functional ones at the same heating rate. Therefore, they are more stable than the OH counterparts. The average activation energies (E_a) of thermal degradation of OH and COOH functional polymers were also determined using Ozawa's and Reich's approaches. According to Ozawa's approach, E_a values of OH functional PLs changing between 73.7 kJ/mol and 76.5 kJ/mol while E_a values of COOH functional PLs changing between 77.9 kJ/mol and 81.8 kJ/mol. According to Reich's approach, E_a values of OH functional PLs changing between 67.8 kJ/mol and 70.7 kJ/mol while E_a values of COOH functional PLs changing between 72.2 kJ/mol and 75.8 kJ/mol. Crystallinities of resultant PLs were characterized by X-Ray Diffraction (XRD). From the diffraction line broadening, it was concluded that the OH and COOH functional PLs have the same crystalline structure. However, some differences exist between the crystallite sizes of linear and multi-arm PLs as well as PLs with OH and COOH end-groups.

Keywords: Poly(L-lactide), Thermal Degradation, Ozawa's and Reich's Approaches, Activation Energy, Crystallite Size.

ÖZET

POLİ(L-LAKTİT)LERİN SENTEZİ, KARAKTERİZASYONU, VE TERMAL BOZUNMASI

İLKNUR TUNÇ
Kimya Bölümü Yüksek Lisans
Tez Yöneticisi: Yrd. Doç. Dr. SONER KILIÇ
Haziran 2004

Bu projede 1, 2, 3 ve 4 kollu poli(L-laktit)ler, halka açılması polimerizasyonuyla, alkol ve kalaydioktat varlığında sentezlendi. Oluşan polimerler jel geçirgenlik kromatografisi (GPC) ve nükleer manyetik rezonans (NMR) spektroskopisiyle karakterize edildi. Bu polimerlerin dinamik ısıl bozunması, termogravimetrik analiz yöntemi (TGA) ile çalışıldı. Uç-grupların ısıl bozunmaya olan etkilerini incelemek için hidroksit fonksiyonel polimerler süksinikanhidrit ile reaksiyona sokularak asit fonksiyonel polimerler elde edildi. Asit fonksiyonel polimerlerin hidroksit fonksiyonellere göre daha kararlı olduğu bulundu. Hidroksit ve asit fonsiyonel polimerlerin termal bozunma aktivasyon enerjileri Ozawa ve Reich yaklaşımlarıyla hesaplandı. Ozawa yaklaşımına göre hidroksit fonksiyonel poli(L-laktit)lerin ortalama aktivasyon enerjileri 73.7 ile 76.5 kJ/mol arasında değişirken, asit fonksiyonel poli(L-laktit)lerin ortalama aktivasyon enerjilerinin 77.9 ile 81.8 kJ/mol arasında değiştikleri tespit edildi. Reich yaklaşımına göre ise hidroksit fonksiyonel poli(L-laktit)lerin ortalama aktivasyon enerjileri 67.8 ile 70.7 kJ/mol arasında değişirken, asit fonksiyonel poli(L-laktit)lerin ortalama aktivasyon enerjilerinin 72.2 ile 75.8 kJ/mol arasında değiştikleri tespit edildi. Oluşan poli(L-laktit)lerin kristalitleri X-Işını Kırınımı (XRD) ile karakterize edildi. Kırınım açılarından, polilaktitlerin aynı kristal yapıya sahip olduğu sonucuna varıldı. Fakat, lineer ve çok-kollu polilaktitlerin aynı zamanda hidroksit ve asit fonsiyonel polilaktitlerin kristalit büyüklüklerinde bazı farklılıklar olduğu ortaya çıktı.

Anahtar Kelimeler: Poli(L-laktit), Termal Bozunma, Ozawa ve Reich Yaklaşımları, Aktivasyon Enerjisi, Kristalit Büyüklüğü.

ACKNOWLEDGEMENTS

I gratefully thank my supervisor Asst. Prof. Dr. Soner Kılıç, for his suggestions, supervision, and guidance throughout the development of this thesis.

I would also like to thank Prof. Dr. Vasıf Hasırcı, Prof. Dr. Atilla Aydınlı, Assoc. Prof. Dr. Ömer Dağ, and Asst. Prof. Dr. Dönüş Tuncel, the members of my jury, for reading and commenting on the thesis.

I also would like to thank to my friend Hakan Durmaz from Istanbul Technical University Chemistry Department and Prof. Dr. Olgun Güven for their assistance for the thesis.

I finally would like to thank to my dear husband Celal Alp for his help throughout the development of this thesis.

LIST OF FIGURES

LIST OF TABLES

CHAPTER 1

INTRODUCTION

Poly(L-lactide) or poly(L-lactic acid) (PL) belongs to a group of biodegradable polymers and has received much interest because of its pharmaceutical and environmental applications. They are thermoplastic and easily processed on standard plastic processing equipment to yield molded parts, films, and fibers.

Their homo- and copolymers can be derived from renewable sources with many useful properties such as mechanical strength, transparency, and compatibility. The attraction of polylactide as a material is its ready availability from renewable resources such as corn, sugar, and dairy products (Figure 1.1). It is also easily biodegraded back to lactic acid or recycled to cyclic diesters, lactide [1].

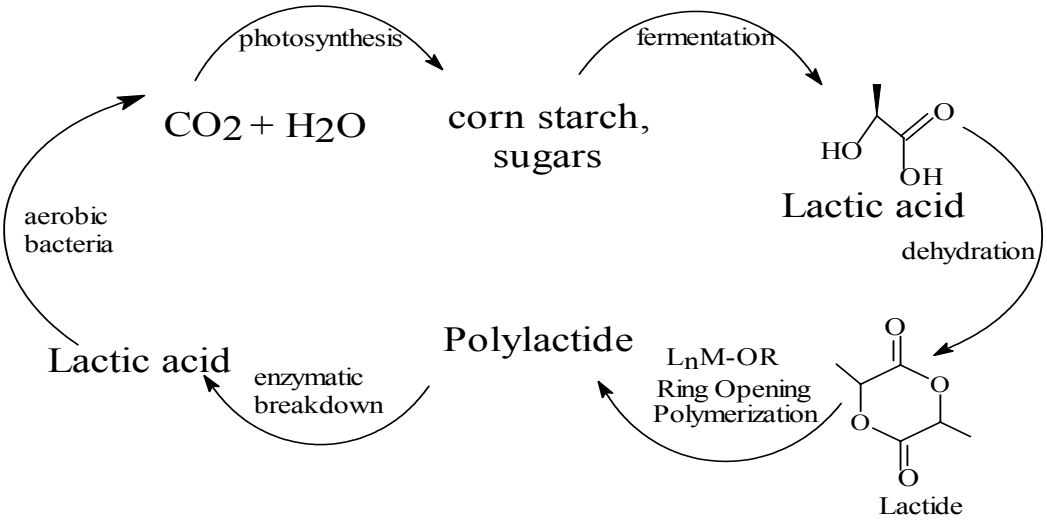

Figure 1.1: Recycle of polylactide in nature.

Lactide is the cyclic dimer of lactic acid that exists as two optical isomers, optically active D- and L-lactide enantiomers, and optically inactive (meso) DL-lactide (Figure 1.2).

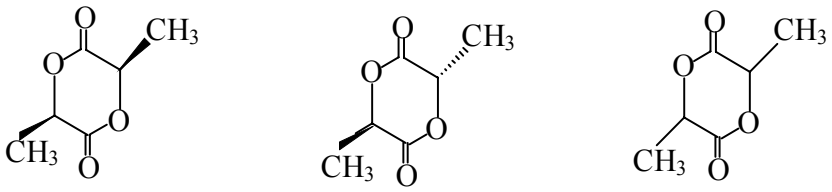

meso-Lactide D-Lactide L-Lactide

Figure 1.2: Structure of D-, L- and meso-lactide.

An optically pure poly(L-lactide) is a crystalline, hard and rather brittle material, melting in the temperature range of 175 – 185°C (depending on the molecular weight and on the size of the crystallites). In contrast, a poly(D,L-lactide) having a random stereosequence is an amorphous transparent material with a glass transition temperature of 50 – 60°C (depending on the molecular weight) [2,3]. Additionally, the amorphous PL is soluble in most organic solvents, such as tetrahydrofuran, chlorinated solvents, benzene, xylene, acetone, acetonitrile, and 1,4-dioxane whereas crystalline PL is soluble in chlorinated solvents, tetrahydrofuran, and 1,4-dioxane at elevated temperatures [4].

PL homopolymers have a very narrow processing window and a major problem in the manufacturing of polylactide products is the limited stability during the melt processing. Polylactides undergo thermal degradation at temperatures above 200°C [5] by hydrolysis, lactide reformation, oxidative chain scission and inter- or intra-molecular transesterification reactions. PL degradation is dependent on time, temperature, low molecular weight impurities, and catalyst concentration [5].

The narrow processing window can be extended by copolymerization. The degree of crystallinity and melting temperature of PL polymers can be reduced by random copolymerization with other comonomers, leading to the incorporation of units disturbing the crystallization ability of the poly(L-lactide) segments [6-10]. For example, D-lactide [6], glycolide [6-8], ε-caprolactone [7,9], and β-methyl-δ-valerolactone [10] have been frequently used as comonomers in order to change the thermal properties of the resulting

PL polymers. Also, the incorporation of such comonomers into a highly crystalline PL generally causes an increase in the biodegradation rate.

Generally, the degradation rate increases with increasing amorphous regions and as molecular weight decreases. Many studies have been carried out to determine the effects of these parameters on polymer degradation rate [11-14]. The end-groups and pH of medium also strongly affect the degradation [11,15]. The effects of all these factors on degradation must be known to control the biodegradation of PLs.

Rheological measurements have proved that the thermal degradation of poly(L-lactide) is accelerated when the moisture content of the polymer is increased and optimal drying conditions have been reported to reduce the degradation during extrusion [4].

The pH is an important factor in the hydrolysis of the polyesters, because hydrolysis is catalyzed by both acid and base. Lee et al. [11] synthesized various end-group-functionalized polylactides and found that the COOH end-group plays a crucial role in the hydrolytic degradation in both alkaline and acidic medium. Protection of OH end-group results in a substantial retarded degradation [16]. It was also reported [16] that the multi-armed structure can increase the end-group effect because of higher end-group concentration than linear polymers of the same molecular-weight.

Our main objective was to prepare linear and multi-armed poly(L-lactide)s (PLs) with OH and COOH end-groups and determine their effects on thermal degradation of these polymers. The OH functional PLs were synthesized by the ring opening polymerization method using tin octoate as a catalyst and the COOH functionalized PLs were prepared by reacting OH functionalized PLs with succinic anhydride. Also, the effects of these end-groups on the crystallite sizes were investigated.

The thesis presents a literature review in the next chapter, i.e., Chapter 2 that summarizes the synthesis and effect of various parameters on synthesis of polylactides. It

also includes effect of some parameters on degradation, biodegradation, hydrolytic degradation, and thermal degradation of these polymers.

The following chapter (Chapter 3) details the synthesis and characterization methods utilized in this project.

Chapter 4 gives the results of this study and the discussion of the results on the bases of the published literature works. Effects of end-groups and their concentrations on thermal degradation of the prepared poly(L-lactide)s are discussed in this chapter.

The final chapter summarizes conclusions of this work.

CHAPTER 2

LITERATURE REVIEW

2.1. Polylactides

Polylactide and its copolymers are one of the most widely used polymers for biomedical applications, such as surgical sutures [18], drug delivery systems [19], and internal backbone fixation [20]. It is biodegradable and biocompatible and it has excellent shaping and moulding properties.

The general criteria of selecting a polymer for use as a biomaterial, is to match the mechanical properties and the time of degradation to the needs of the application. The factors affecting the mechanical performance of biodegradable polymers are those: monomer and initiator selection, process condition, and presence of additives. These factors in turn influence the polymer's hydrophilicity, crystallinity, melt and glass-transition temperatures, molecular weight, molecular weight distribution, end groups, sequence distribution (random versus block), and presence of residual monomer or additives. In addition, the effect of these variables on biodegradation must be evaluated for biodegradable materials [1].

Biodegradation is accomplished by synthesizing polymer that has hydrolytically unstable linkages in the backbone. The most common chemical functional groups with this characteristic are esters, anhydrides, and orthoesters [21].

Polylactide is generally produced by ring opening polymerization (ROP) of lactide through the lactide intermediate with a variety of organometallic catalysts [22-26]. For commercial production [1], in the first step of the process water is removed under mild conditions (and without the use of a solvent) to produce a low molecular-weight prepolymer. This prepolymer is then catalytically depolymerized to form a cyclic intermediate dimer (Figure 2.1) referred to as lactide which is then purified to polymer

grade using distillation. The purified lactide is polymerized in a solvent free ROP and processed into polylactide pellets. By controlling the purity of the lactide it is possible to produce a wide range of molecular weights.

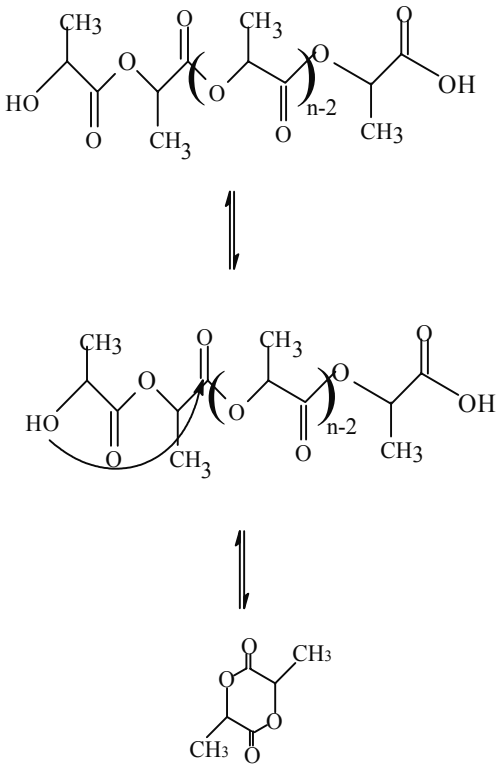

Figure 2.1: Formation of lactide from poly(lactic acid).

The homopolymer of L-lactide is a semicrystalline polymer. Poly(L-lactide) is widely studied for possible biomedical applications, particularly for those that demand good mechanical properties for surgical sutures and devices for internal bone fixation [27-29].

Poly(DL-lactide) is an amorphous polymer exhibiting a random distribution of both isomeric forms of lactide and accordingly is unable to arrange into an organized crystalline structure. This material has lower tensile strength, higher elongation, and a much more

rapid degradation rate. Poly(L-lactide) is about 70% crystalline, with a melting point of 175-178^{o}C and a glass transition temperature of 60-65^{o}C [2,3]. The degradation rate of poly(L-lactide) is much slower than that of poly(DL-lactide). Copolymers of L-lactide have been prepared to decrease the crystallinity of L-lactide and accelerate the degradation process.

Until 1995, it was believed that a high molecular weight of polylactide could not be prepared by the direct polycondensation of lactic acid because of the difficulty in driving the dehydrative equilibrium in the direction of esterification or the formation of polylactide with sufficiently high molecular weight. Later, Mitsui Chemicals developed a new process based on direct polycondensation of L-lactic acid to enable the production of high molecular weight poly(L-lactide) without the use of an organic solvent [1].

2.2. Synthesis of Polylactides

Polylactide can be synthesized by two different pathways: either the step polycondensation of lactic acid; or the ring opening polymerization of the cyclic diester, lactide. In contrast to the more traditional polycondensation, that usually requires high temperatures, long reaction times and a continuous removal of water, to finally recover quite low molecular weight polymers with poor mechanical properties, ROP of lactide provides a direct and easy access to the corresponding high molecular weight polylactide. The ring opening polymerization of lactide is known to be promoted by Lewis acid type catalysts. It is initiated by protonic compounds such as water, alcohols, thiols, metals, metal halogenides, oxides, aryls and carboxylates. The main representative of this group of catalysts is tin(II) bis(2-ethylhexanoate) ($Sn(oct)_2$ or tin octoate) [3,30,31].

There are also some articles which detail the studies on the usage of tertiary amines [32], phosphine [33], and N-heterocyclic carbenes [34] as nucleophilic organic catalyst for the control ROP of lactides.

In the literature, two major ROP mechanisms are proposed: the activated monomer mechanism [35] and the coordination-insertion mechanism [22,36]. Both mechanisms are thought to be alcohol-initiated since the degree of polymerization is clearly dependent on the monomer-to-alcohol ratio, and the end-groups of the polymer have hydroxyl functionalities. The coordination-insertion mechanism provides an explanation of the highly-stereoregular polymers obtained with tin octoate.

2.2.1. Activated Monomer Mechanism

In the activated monomer mechanism [35], tin octoate forms a donor-acceptor complex with a monomer. This activates the monomer toward alcohol attack. A hydroxyl-ended macromolecule attacks the carbonyl carbon and ring-opening proceeds. In other words, initiation and polymerization proceed by an ester alcoholysis reaction mechanism, in which the tin octoate activated ester groups of the monomers react with hydroxyl groups. The activated monomer mechanism is outlined in Figure 2.2.

In this mechanism, the tin atom of tin octoate coordinates with the carbonyl oxygen atom of the lactide (**1**). Due to the coordination with tin the carbonyl carbon atom becomes more positive (**2**), resulting in an increased susceptibility to nucleophilic attack by a hydroxyl group (**3**). In the initiation reaction, the hydroxyl group containing compound is the added alcohol, whereas in the propagation reaction the hydroxyl group is the end-group of a growing polymer chain.

After proton transfer (**4**) and the actual ring-opening of the monomer by acyl-oxygen cleavage (**5**), a linear molecule with an alcohol-derived ester end-group and a lactide-derived hydroxyl end-group is formed. The ester of the ring-opened monomer still coordinated to the tin atom exchanges with a second monomer molecule, whereafter the process starts again at **1**. Consequently a tin octoate molecule is not bound to one particular polymer chain, but constantly changes from one to another growing polymer chain. Therefore the molecular weight of the polymer will not be determined by the tin octoate concentration, but by the hydroxyl group concentration only.

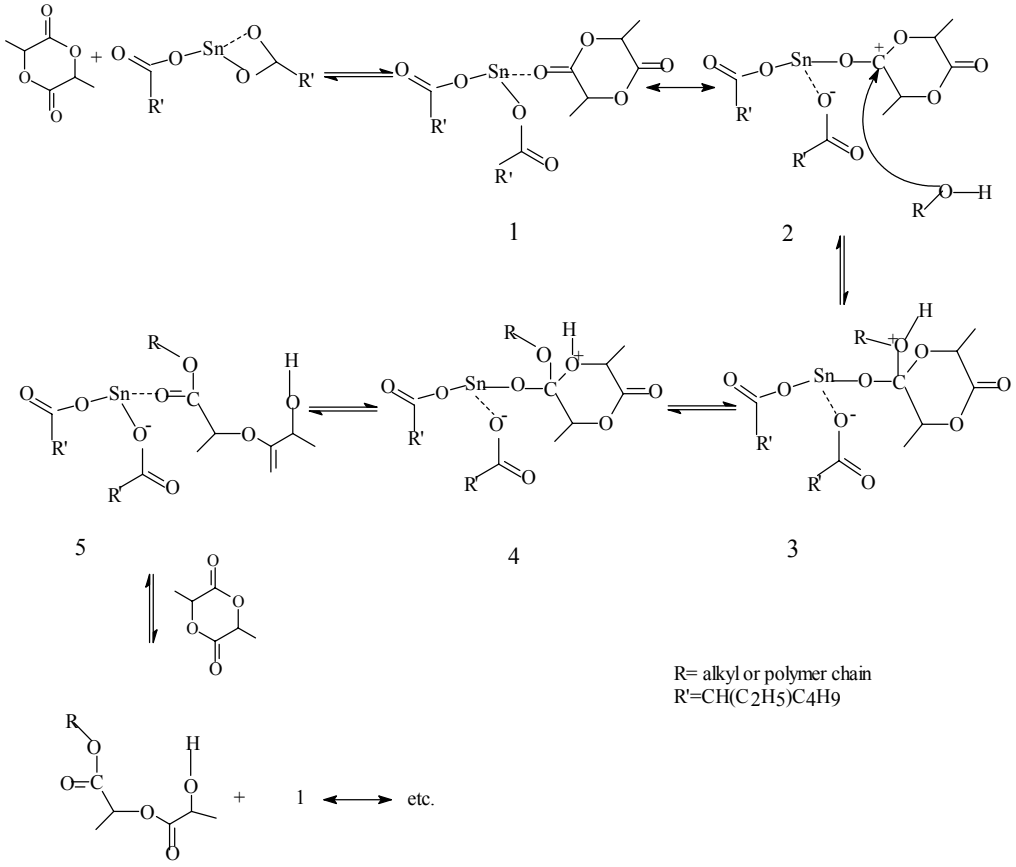

Figure 2.2: Activated monomer mechanism of ROP of L-lactide with tin octoate.

2.2.2. Coordination-Insertion Mechanism

In the coordination-insertion mechanism [22, 36], a compound containing a hydroxide group is believed to react with tin octoate to form the actual initiator, i.e., an alkoxide covalently bound to tin. The coordination-insertion mechanism involving the ROP of L-lactide with tin octoate is depicted in Figure 2.3. A stable complex was formed with alcohol coordinating to tin octoate prior to the actual ring-opening sequence. The first step involved coordination of alcohol to tin octoate (**6**) to form structure **7**. As the alcohol coordinated to tin, a hydrogen bond was simultaneously formed to the carbonyl oxygen atom of the octoate ligand. A second alcohol coordinated to **7** to form structure **8**.

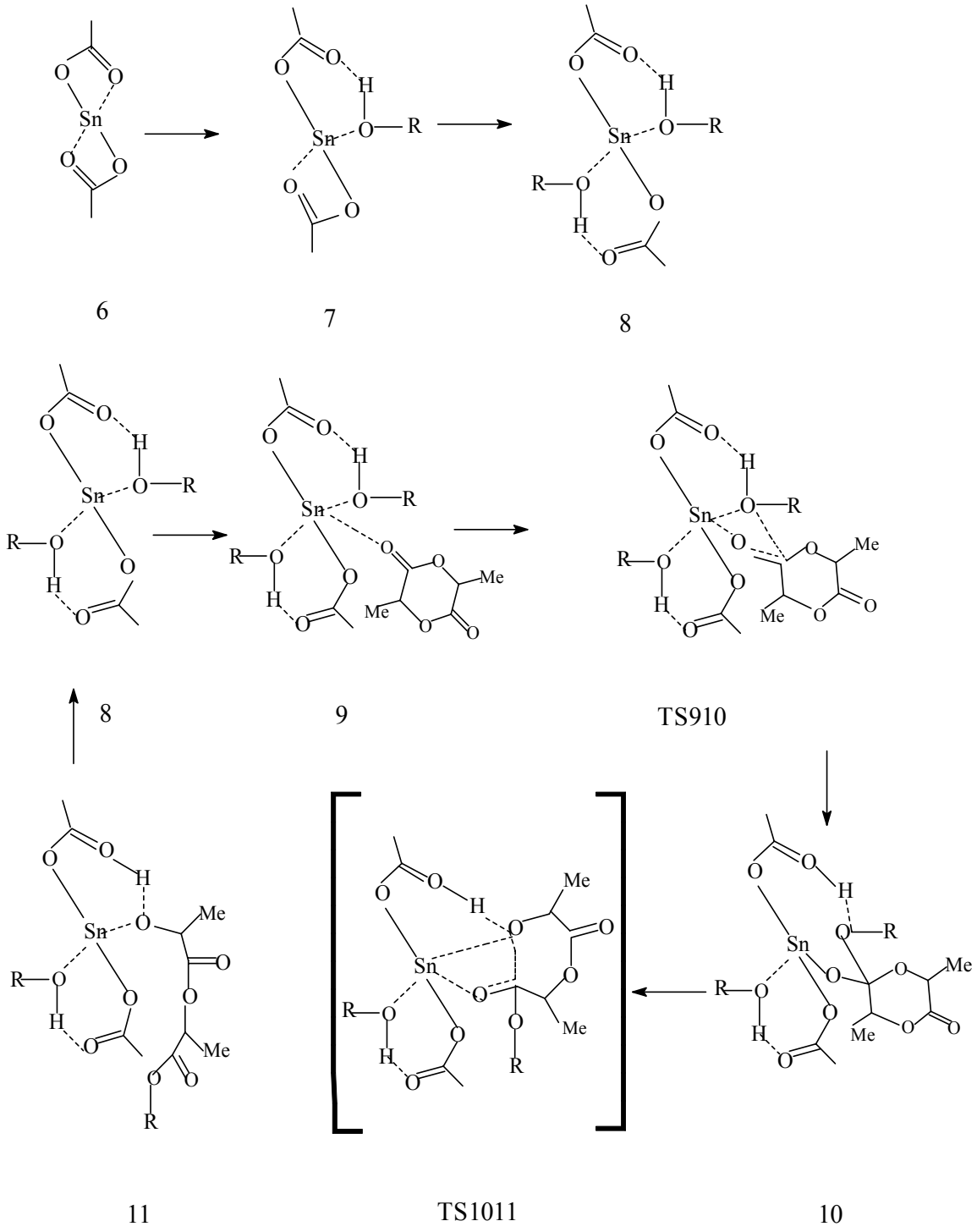

Figure 2.3: Coordination-insertion mechanism of ROP of L-lactide with tin octoate.

The initial step involved the weak complexation of monomer to complex (**8**). Although weak, coordination of the monomer had an important influence on the chemical nature of the ligand structure. Proton migration was induced from the alcohol to the near by octoate ligand. Consequently, the octoate ligand took on the character of a carboxylic acid, while the alcohol was converted into an alkoxy-type species. The ligand retained its character throughout step **9** to **TS1011**, stabilizing these structures through hydrogen bonding. After precursor **9** was formed, the methoxy group performed a nucleophilic attack on the monomer's carbonyl carbon, and a new C–O bond was formed between monomer and methoxy group via the four-center transition state **TS910**. The next step in the mechanism was the actual ring opening of the monomer, **10** to **11**. In the intermediate **10**, the former carbonyl oxygen is coordinated to tin via an alkoxide bond. This arrangement allows for the rotation around C–O axis and enables the endocyclic oxygen to rotate into the position for ring opening. **TS1011** was four-centered transition state and structurally analogous to **TS910**, although the bonds formed in **TS1011** were the bonds broken in **TS910**. The alcohol of the ring-opened monomer still coordinated to the tin atom exchanges with a second molecule, where after the process starts again at **8**.

2.2.3. Effect of Various Parameters

2.3.3.1. Catalyst

For commercial production, it is preferable to carry out bulk melt polymerizations that use lower levels of non-toxic catalysts. Tin octoate is preferred for three reasons [30, 31, 37-40]. First, tin octoate is a highly efficient catalyst and allows almost complete conversions even at monomer-to-catalyst ratios as high as 10,000. Second, the risk of racemization is low, and 99% optically pure poly(L-lactide) can be prepared even at 150^{o}C, when the reaction time is limited to a few hours. Third, tin octoate is a permitted food additive which means that its toxicity is extremely low compared to other heavy metal salts [37].

Kricheldorf and Serra [37] screened 24 different oxides, carbonates, and carboxylates of tin, zinc, aluminum, and other heavy metals as catalyst in the bulk polymerization of lactide at 120, 150, and 180^{o}C. They found that the most effective catalysts in terms of yield, molecular weight, and racemization were tin(II) oxide and octoate at 120 – 150^{o}C. Few carbonates yielded acceptable polymerization, however, all had considerable racemization. In another study [41], it was reported that the catalytic effect of alkali and alkaline earth metal carboxylates such as sodium and calcium carboxylates were similar to the carbonates.

2.2.3.2. Temperature and Time

Witzke et al. [31] studied the ROP of L-lactide in the presence of tin octoate as a catalyst over a wide range of temperatures (130 – 220^{o}C) and monomer to catalyst molar ratios, M/C, (1,000 – 80,000). It was reported that the conversion and number-average molecular weight increased with polymerization time and temperature. It was also found that the conversion is a function of M/C ratio. At 130^{o}C, greater than 90% conversion was obtained in 5 hours at M/C < 3,000, whereas it took about 40 hours for M/C ≈ 20,000. At higher temperatures (220^{o}C), greater than 90% conversion was obtained in about 40 hours at M/C < 40,000. It was also reported that the racemization was a significant side reaction during the polymerization in this temperature range. The effects of polymerization temperature and time on the catalyzed polymerization were also studied by others [37, 42]. Schwach et al. [42] found that the yield and transesterification is affected, by polymerization temperature > M/C > polymerization time > type of catalyst > monomer degassing time and pressure, in the following order.

2.2.3.3. Crystallinity

Nijenhuis et al. [40] found that the rates of chain growth vary greatly in a polymerization catalyzed with tin octoate and depend not only on impurities but also on the formation of crystalline phases during polymerization. The apparent rate of propagation will increase and the apparent equilibrium monomer concentration will decrease when

crystalline polymer domains form during polymerization. They showed that when L-lactide is polymerized below the polymer crystalline melting temperature, crystalline domains form that exclude both monomer and catalyst. This constant enrichment of the amorphous phase leads to higher polymerization rates. The apparent equilibrium monomer concentration is reduced due to lower percentage of amorphous to crystalline phase in the total system. The apparent equilibrium monomer concentration is in direct proportion to the degree or percent of amorphous phase in the polymer.

2.2.3.4. Impurities

The polymerization rate and molecular weight were affected by addition of hydroxylic or carboxylic impurities. The addition of lactic impurities (i.e., water, lactic acid) does not significantly affect the polymerization rate, but the final molecular weight [40]. This was theoretically due to the presence of both hydroxyl and carboxyl groups. However, the addition of free carboxylic acids has an inhibitory effect on the polymerization rate but does not affect the final molecular weight. This might have been due to free acids, which do not react with the lactide preferentially but complex with the catalyst and lower its catalytic activity. Hydroxylic impurities, which increased the rate of polymerization in proportion to their concentration and also directly control the final molecular weight, had opposite effect. This would point out that the hydroxylic compounds interact with both the catalyst and lactide. Alcoholic initiators could react with the tin octoate to produce more active catalyst.

Tin octoate catalyzed transesterification reaction of lactone and lactides to produce stereoregular polymer of high molecular weight and at high yields [43]. In that article, they concluded that, the determination of reaction mechanism was very difficult by kinetic studies or from analysis of end-groups and reaction products. It was also concluded that, the explanation of the structure of the actual initiating and propagating species of ROP by spectroscopic and chromatographic methods was difficult.

2.3. Stability and Degradation

Stability is important for biomedical polymers in most clinical applications. However, degradation might be a preferable property as well. According to this circumstance the control of the degradation of biomaterials becomes critical for completion of the assigned function.

The degradable polymer serves only a temporary function after the tissue or organ has healed successfully it should degrade to harmless compounds which can be resorbed or excreted by the body. In order for the polymer to degrade *in vivo*, the polymers to be used should contain hydrolytically unstable chemical bonds in the main chain. Such polymers are polyesters, polyethers, polyurethanes, polycarbonates, polyanhydrides and copolymers of these [21, 43-46]. The rate of degradation of the polymer is dependent on the ease of hydrolyzability as well as on the accessibility of this unstable bond to enzymes and water. The hydrophilicity of the material, the morphology and crystallinity of the polymer, and its molecular weight are important parameters determining the degradability as well as the mechanical properties [47,48].

To initiate the degradation process, polymers which has strong bonds in the backbone and no easily hydrolyzable groups need long times, activators or catalysts. These initiating factors could be heat, electromagnetic radiation such as visible light, UV, gamma, chemicals like water oxygen, ozone and halogenated compounds or any combination of above. The molecules with such hydrolyzable groups are degradated much more efficiently and rapidly [14].

Polymers can degrade through the breakage of end units on the chain (unzipping) or through scission of a bond along the length of the polymer backbone (random scission). Backbone breakage is encouraged as penetration capacity of a solvent into polymeric form is increased. In other words, biodegradability increases with increasing hydrophilicity of polymer. Chain scission may not be without side reactions. Gogolewski and Varlet [49] reported that polyhydroxyacids can undergo chain scission at the ester bond followed by

new bond formation on transesterification. It would lead to molecules which are longer than the starting materials.

PLs undergo thermal degradation at temperature above 200^{o}C by hydrolysis, lactide reformation, oxidative main chain scission, and inter or intramolecular chain transesterification reactions. PLs degradation depends on time, temperature, low-molecular weight impurities, and catalyst concentration. Catalyst and oligomers decrease the degradation temperature and increase the degradation rate of PLs [5].

2.3.1. Biostability and Biodegradation

Biodegradation has been defined as "the gradual breakdown of material mediated by specific biological activity" [50]. This process may be initiated and maintained by enzymes or microorganisms and include abiotic reactions like hydrolysis and/or oxidation, which result in a fragmentation of the molecules.

Biodegradable polymers are defined as those which are degraded in biological media where living microorganism, cells are present, such as soil, compost, seas, rivers, lakes, body of human and animals. That biodegradation can be enzymatic or non-enzymatic hydrolysis is a complex process including chemical and biological reactions, which occurs simultaneously [50].

The biodegradation of lactic acid based polymers have previously been included in several reviews [4,14].

Polymer degradation occurs mainly through scission of the main chains or side chains of macromolecules. In nature, polymer degradation is induced by thermal activation (i.e. enzymes), oxidation, photolysis or radiolysis [51].

Besides environmental conditions such as pH, temperature, phase, exposure, mechanical stress and biological activity, polymer degradation is also dependent on the

chemical and physical characters of the polymer. They are diffusivity, morphology, cross linking, purity, chemical reactivity, mechanical strength and thermal tolerance [51].

The biodegradation of lactic acid based polymers for medical applications has been investigated in a number of studies *in vivo* [52-54] and some reports can also be found on the degradation in other biological systems [2,55,56]. A screening study, where the degradation of poly(L-lactide) in presence of a number of different enzymes, was reported by Shirama et al. [57].

The mechanism of PLs is dependent on biological environment to which they are exposed. In mammalian bodies PL is initially degraded by hydrolysis and then formed oligomers are metabolized or mineralized by cells and enzymes. Abiotic hydrolysis is known as initial stage of degradation before microbial biodegradation of PL occurs in nature. However, degradation rate increases in the compost environment in the presence of an active microbical community comparing to the abiotic hydrolysis. The environmental degradation of PL occurs by two-step process. During the first phases of the degradation, the high molecular weight polyester chains hydrolyze to low-molecular-weight oligomers. The reaction can be accelerated by acids or bases and is affected by both temperature and moisture levels. At number average molecular weight 10,000 and 40,000 Da, microorganisms in the environment continue the degradation process by converting these low molecular weight components to carbon dioxide, water, and humus [2,58].

The effect of molar mass of poly(L-lactic acid), ranging from 26,000 to 288,000 Da, on the biodegradation has been studied by Karjomaa et al. [59]. The degradation rate was found to decrease with increasing chain length and proceed somewhat more rapidly in biotic environment. The effects of physical ageing and morphology on the enzyme degradation of poly(L-lactic acid) were studied by Cai et al. [60]. It was concluded that morphological changes due to the ageing affect the rate of degradation by reducing the mobility of the polymer chains, which was reflected in a lower degradation rate.

Combinations of lactic acid based polymers and different low or high molar mass compounds have been found to affect the degradation behavior. The presence of lactic acid and lactoyllactic acid was demonstrated to increase the biotic degradation of poly(L-lactide) [61]. The presence of poly(*rac*-lactide) and poly(D-lactide) has also been reported to affect the biodegradation [62].

2.3.2. Hydrolytic Degradation

Hydrolysis of polymers leads to molecular fragmentation, which can be regarded as a reverse polycondesation. These processes can be affected by various factors such as chemical structure, molar mass and its distribution, purity, morphology, shape of specimen and history of polymer, as well as the conditions under which the hydrolysis is conducted [63]. The hydrolytic degradation of lactic acid based polymer is a phenomenon, which is undesired, at certain circumstances, e.g. during processing or material storage, but beneficial in other applications, for example, in medical devices or compostable packages. The hydrolysis of aliphatic polyesters starts with a water uptake phase followed by hydrolytic splitting of the ester bonds in random way according to the Flory principle, which postulates that all linkages have the same reactivity. This was demonstrated by Shih [64] who reported on random scission during alkali hydrolysis of poly(*rac*-lactide) when acid catalyzed hydrolysis gives the faster chain end scissions. The latter phenomenon can be explained by a growing amount of chain end, which with the time leads to an increased probability of breaks at the chain ends. The initial degree of crystallinity of the polyester affects the rate of hydrolytic degradation as the crystal segments reduce the water permeation in the matrix.

The amorphous parts of the polyesters have been noticed to undergo hydrolysis before the crystalline regions because of a higher rate of water uptake. The first stage of the hydrolytic degradation is accordingly located to the amorphous regions where the molecular fragments that are tying the crystal blocks together by entanglement, are hydrolyzed. The remaining undegraded chain segments therefore obtain more space and

mobility, which lead to reorganizations of the polymer chains and an increased crystallinity [65].

The temperature during the hydrolysis is of major importance for the degradation rate. This is not only because of an increased hydrolysis rate at elevated temperature, but also a result of the flexibility of the polymer when the temperature is above the glass transition temperature of the polymer [66].

The hydrolysis of lactic acid based polymers has been studied for different composition: poly(L-lactide) [7,67], poly(*rac*-lactide) [7,68], poly(L-lactide-co-glycolide) [7,69], poly(*rac*-lactide-co-ε-caprolactone) [7,70]. In addition, the hydrolytic degradation for poly(L-lactide)s of different molar mass as well the hydrolytic degradation of high molar mass poly(ester-urethanes) prepared from lactic acid have been reported [71].

The hydrolytic degradation of blends of aliphatic polyesters has been studied for poly(L-lactide-co-glycolide) in blends with poly(ε-caprolactone) and poly(L-lactide) [72]. The ways of preparing the blends were compression molding, coprecipitation and solvents-water emulsion of the polymers. The type of blending method was found to affect the ratio of the chain-scission rate between the blending components.

The hydrolytic degradation of the PL homo- and copolymers is homogeneous, i.e. the number-average molar mass has significantly decreased before any weight loss can be noticed. In the second stage of hydrolysis the hydrolytic degradation of the crystalline regions of the polyester leads to an increased rate of mass loss and finally to complete resorbtion. The degradation of PL in aqueous medium was reported [73] to proceed more rapidly in the center of specimen. The explanation to this behavior was an autocatalytic effect due to increasing amount of compounds containing carboxylic end-groups. These low molecular mass compounds were not able to permeate the outer shell. In contradiction, the degradation products in the surface layer were continuously dissolves in the surrounding buffer solution.

The influence of peroxide-modification on the hydrolytic degradation has been studied in another study [74]. It was reported that the weight loss, the decrease of the tensile strength, and the decrease in molar mass were more apparent for the peroxide modified poly(L-lactide) than for the unmodified.

2.3.3. Thermal Stability and Degradation

The thermal stability of aliphatic polyesters is in general limited [75-77]. The thermal stability of lactic acid based polymers is accordingly poor at elevated temperatures, and most of the reported studies are mainly concerned with the degradation of poly(L-lactic acid), poly(L-lactide), and poly(*rac*-lactide). In one of these reports, Gupta and Deshmukh [77] concluded that the carbonyl carbon-oxygen linkage is most likely one to split by isothermal heating. Significantly larger amount of carboxylic acid end-groups than hydroxyl end-groups was identified, which indicated a break of the carboxyl carbon-oxygen linkage. In another report, it was concluded that the kinetics for the thermal degradation of lactic acid suggested as being first order [72]. In terms of degradation mechanism, there are various suggestions for lactic acid based polymers which are: thermohydrolysis [78], zipper-like depolymerization [5,79], thermo-oxidative degradation, [31] and transesterification reactions [5,80].

Poly(*rac*-lactide) is a highly hygroscopic polymer which has been reported to absorb water [73]. Semicrystalline poly(L-lactide), on the other hand tends to increase its weight by water uptake with only some few percents [74]. Rheological measurements have proved that the thermal degradation of poly(L-lactide) is accelerated when the moisture content of the polymer is increased [4] and optimal drying conditions have been reported to reduce the degradation during extrusion. On the other hand, other studies have shown that the extent of the thermal degradation between carefully dried and undried PLLA did not vary [5].

Zipper-like depolymerization of the polymer, in the presence of the catalyst, has been proposed to be a significant mechanism in the degradation of polylactide. A

mechanism for this biting depolymerization of tin octoate has been suggested by Zhang and Wyss [79]. The presence of catalyst, especially the catalyst concentration, is of great importance for the thermal stability of polylactide. A strong correlation between catalyst amount added and degradation rate has been reported [5, 79]. Purification of the polymer in order to decrease the catalyst content caused a retardation of thermal degradation. However, the purification did not only remove the non-bound catalyst but also residual monomer and other impurities, which have been reported to have an influence on the thermal stability [17]. Thermooxidative random main scission was proposed as one contributing mechanism to the thermal degradation of polylactide by McNeill and Leiper [81] as well as Gupta and Deshmuk [77]. The presence of oxygen has been noticed to have slightly stabilizing effect on poly(L-lactide) during the first minutes of melt processing [5]. This was explained by means of a prevented depolymerization due to a deactivation of the catalytic tin present in polylactide prepared in a tin(II) 2-ethylhexanoate catalyzed ROP. Inter- and intramolecular transesterifications, including acidolysis and alcoholysis, are typical interchange reactions for condensation polymers above and near their melting points [82]. Kinetic studies have shown that the mechanism of transesterifications is an associative-type mechanism, where breaking and making of bonds occur simultaneously. Interchange reactions in polyesters are rapid in the melt, but they also take place below the melting point of the polymer [83]. By using ion mass spectroscopy for analysis of pyrolyzed polylactide, ring structures of various sizes were found. Any increase in the amount of end-groups could not be noticed, which was explained by the formation of cyclic oligomers and monomer by transesterification reactions in the polylactide. McNeill and Leiper [81] and Jamshidi et al. [5] suggested an ester interchange degradation mechanism where hydroxyl end-groups are involved. They performed experiments where the amount of hydroxyl end-groups was reduced by acetylation, which proved to reduce the melt degradation significantly.

2.3.3.1. Kinetics of Thermal Degradation

Various kinds of materials have been studied by thermogravimetric analysis, in which the weight change of a sample heated isothermally or at a constant rate of heating (dynamic) is recorded. Dynamic Thermogravimetry has an advantage over measurement at a constant temperature, because in the latter, a part of the sample may change while the sample is heated to the desired temperature. Especially at the degradation of polymers with high molecular weight, this initial structure change in the sample complicates the isothermal data and makes it difficult to analyze.

Thermogravimetric analysis is widely used as a fast and exact method for the degradation of polymers. Conversion of data from raw thermograms into kinetic parameters such as activation energy, preexponential (frequency) factor, reaction order, and rate constant is based on the utilization of classical laws of kinetics. A number of methods for the calculation of kinetic parameters have been developed. Detailed descriptions of methods are not given here, since there is an abundance of literature on the subject [84-89].

The isothermal rate of conversion, $d\alpha/dt$, in the process of thermal degradation is generally expressed by

$$d\alpha/dt = k\, f(\alpha) \qquad (2.1)$$

The conversion is defined by

$$\alpha = 1 - W/W_o \qquad (2.2)$$

where W_o and W represent initial weight and weight at any time, respectively. In Equation (2.1), the rate constant *k* depends on temperature *T* according to the Arrhenius relationship

$$k = A \exp(-E/RT) \qquad (2.3)$$

where R is the gas constant, A is preexponential (frequency) factor, and E is energy of activation.

On the other hand, $f(\alpha)$ is a function of conversion and is expressed in analogy to simple cases in homogenous kinetics as

$$f(\alpha) = (1- \alpha)^n \qquad (2.4)$$

where n is the apparent order of reaction. Substitution of Equations (2.3) and (2.4) into Equation (2.1), gives

$$d\alpha/dt = A\ (1- \alpha)^n \exp(-E/RT) \qquad (2.5)$$

Experiments in thermal analysis are carried out isothermally or at a constant rate of heating B = dT/dt. In the latter case, Equation (2.5) can be written in the form;

$$d\alpha/dT = (A/B)\ (1- \alpha)^n \exp(-E/RT) \qquad (2.6)$$

Determination of parameters A, E, and n is based on the solution of Equations (2.4) and (2.6). Generally, the methods that have been developed to calculate the kinetic parameters can be divided into two groups depending whether integral or differential forms of Equations (2.1), (2.5), and (2.6) are used. The basic equations derived by Ozawa [86] and Reich [87] for integral methods are:

Ozawa:

$$E = \frac{R\ \log(B_2/B_1)}{0.457\ (1/T_1 - 1/T_2)} \qquad (2.7)$$

Reich:

$$E = \frac{R\ \ln\left[(B_2/B_1)(T_2/T_1)^2\right]}{(1/T_1 - 1/T_2)} \qquad (2.8)$$

CHAPTER 3

EXPERIMENTAL

3.1. Materials

L-lactide was purchased from Aldrich and was purified by recrystallization from dry ethyl acetate and dried for 24 hours at 30^{o}C *in vacuo* before use. Stannous octoate and triethylamine (TEA) were purchased from Aldrich and were used as catalysts without further purification. Dodecanol, ethyleneglycol, trimethylolpropane and pentaerythritol were purchased from Aldrich and were used as initiators. Succinic anhydride was purchased from Aldrich and was used as received without further purification. All other chemicals and solvents were analytical-grade and were used without further purification.

3.2. Characterizations

The structure of the polylactides was analyzed with a Bruker 250 MHz ^{1}H NMR in deuterated chloroform solution at ambient temperature. Tetramethylsilane signal is taken as the zero chemical shifts. The average molecular weights (Mn and Mw) and the distributions (Mw/Mn) were determined by gel permeation chromotography (GPC) on a Agilent 1100 unit equipped with Waters pump and three Waters styragel HR3, HR4, and HR4E columns using tetrahydrofuran as the eluent at a flow rate of 1 mL/min at 30^{o}C, and the detection was carried out with a differential refractometer. Molecular weights were calculated by using polystyrene standards. To study the thermal degradation of polylactides, two different instruments were used, one of which was Setaram TG-DTA/DSC Labsys Model Thermogravimetric Analyzer (TGA) and the other one was Dupont 951 TGA. The latter was calibrated using calcium oxalate and both instruments gave reproducible results for the same PL sample.

The XRD patterns of powdered samples were recorded on a Rigaku Miniflex diffractometer using a high power Cu-Kα source operating at 30 kV/15 mA.

3.3. Synthesis of Poly(L-lactide)s

3.3.1. Synthesis of OH-Terminated Poly(L-lactide) (OH-PL)

To synthesize the one-armed PL, L-lactide (2.5 g 17.3 mmol) and 1-dodecanol (0.018 g 0.099 mmol) were added in a 50 mL round bottom flask containing a Teflon coated magnetic stirring bar, N_2 inlet, thermometer, and a condenser. The flask was placed in a silicone oil bath and heated to the polymerization temperature (135^{o}C). Before addition of the catalyst, stannous octoate (0.0208 g 0.05 mmol), the reaction mixture was held about six hours at 135^{o}C. Then, tin octoate was added into reaction medium and the polymerization reaction continued further for six hours. The solid was dissolved in 10 ml chloroform and then the polymer was precipitated by adding the polymer solution dropwise into 100 ml methanol. The solid was filtered and dried for overnight at 60^{o}C *in vacuo*. The yields of products are 84, 75, 85, and 80 percent respectively for 1, 2, 3, and 4-armed OH PLs. For the synthesis of 2, 3 and 4-armed OH PLs at the same number average molecular weight of 1-armed OH PL, dodecanol was replaced by calculated amount of ethylene glycol, trimehylolpropane and pentaerythriol, respectively. The procedure of Lee et al. [11] was modified in order to obtain the best synthesis conditions.

The linear and multi-armed OH-PLs were analyzed for end-groups with a Waters 250 MHz ^{1}H-NMR spectrometer in deuterated chloroform ($CDCl_3$). The assignments of the peaks are as follow:

δ=5.18 ppm {nH,q,[OCO-(CH)OCO]}; δ=4.38 ppm {1H,q,[OCO(CH)OH]}; δ=4.17 ppm {2H,t,[C(CH_2)OCO)]}, δ=1.59 ppm {3nH, d, (CH_3)}].

3.3.2. Synthesis of COOH-Terminated Poly(L-lactide) (COOH-PL)

In order to prepare COOH functionalized PL, 1 g of OH functional PL, succinic anhydride amount of which is arranged according to molecular weight of the hydroxyl funtionalized PL, and 0.065 g of triethylamine (TEA) as a catalyst were dissolved in 1, 4-

dioxane and and th resulting solution was stirred for four days at room temperature. Then major part of 1, 4-dioxane was removed using rotary evaporator, and the residue was dissolved in chloroform. The dissolved residue was added into an excess amount of methanol (100 ml) to form precipitate which were filtered through suction, and dried for overnight at 60^{o}C *in vacuo*.

The assignments of the peaks from the ^{1}H-NMR spectrum of 1 COOH PL are as follow:

δ = 5.18 ppm {nH,q,[OCO-(CH)OCO]}; δ = 2.68 ppm {4H, t ,[OCO(CH_2CH_2)-COOH]}; δ = 4.17 ppm {2H, t, [C(CH_2)OCO)]}; δ = 1.59 ppm {3nH, d, (CH_3)}].

CHAPTER 4

RESULTS AND DISCUSSIONS

4.1. Synthesis of Poly(L-lactide)s and Their Characterization by GPC

The linear and multi-armed OH-PLs were synthesized by ROP using L-lactide and various kinds of alcohols in the presence of tin octoate. All the polymerizations were carried out in bulk with continuous stirring. The overall reactions for the synthesis of OH functional PLs are depicted in Figure 4.1.

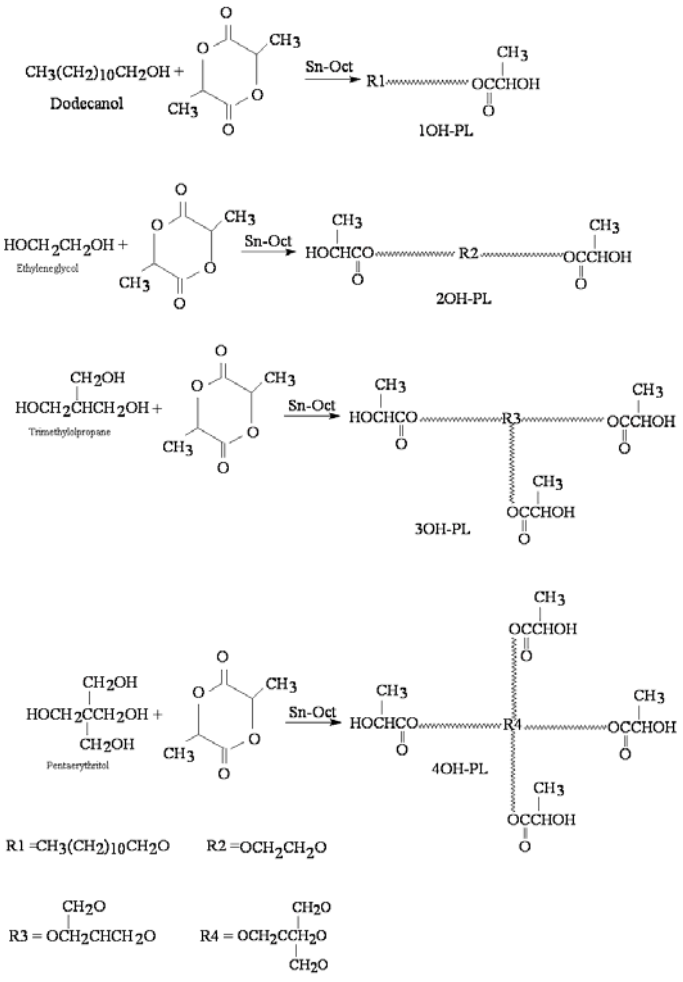

Figure 4.1: Synthesis of 1, 2, 3 and 4-armed OH-PL.

The number-average molecular weight ($M_{n,GPC}$), weight-average molecular weight ($M_{w,GPC}$) and molecular weight distributions or polydispersity (PD_{GPC}) of the resultant polymers were obtained by GPC and are tabulated in Table 4.1 together with their theoretical number-average molecular weights ($M_{n,theo}$). The yield percentages in Table 4.1 were determined gravimetrically as follows:

$$\text{Yield (\%)} = [W_p / (W_m + W_a)] \times 100 \qquad (4.1)$$

where W_p represents the weight of dried polymer and W_m and W_a are the weight of the L-lactide and alcohol initially charged in the reactor, respectively.

Table 4.1: Molecular weights of OH functional PLs determined by GPC and ^{1}H-NMR

	$M_{n,theo}$	$M_{n,NMR}$	$M_{n,GPC}$	$M_{w,GPC}$	PD_{GPC}	Yield (%)
1-armed OH PL	**25,400**	**19,500**	**19,900**	**29,600**	**1.49**	**84**
2-armed OH PL	**25,300**	**18,300**	**18,900**	**28,700**	**1.52**	**75**
3-armed OH PL	**25,300**	**18,900**	**19,200**	**32,900**	**1.71**	**85**
4-armed OH PL	**25,300**	**18,100**	**18,400**	**27,600**	**1.50**	**80**

The molar ratios of the L-lactide to alcohol in resultant OH-PLs which are depicted in Table 4.1 were adjusted to yield about the same molecular weights of PLs. The theoretical M_n values calculated to be around 25,300 Da using the molar ratio of L-lactide to alcohol as 175:1. The M_n values were chosen to be about the same for linear and multi-armed OH-PLs to eliminate the effects of molecular weight difference for the degradation and crystallinity studies. Also, for the end-group characterization by ^{1}H-NMR, the M_n values were chosen to be around 25,300 Da. The experimental number-average molecular weights ($M_{n,GPC}$) were found to be in the range of 18 – 20,000 Da which are somewhat less than the theoretical values. These lower molecular weights may be because of the lower conversion of monomer to polymer. The lower conversion may be related to short polymerization time and/or the presence of some impurities. The molecular weight

distributions were in the range of 1.49 – 1.71, implying that the polymerization mechanism in the presence of tin octoate is not a cationic, anionic, or pseudoanionic mechanism [30]. Kricheldorf et al. [30] proposed a complexation or second-order insertion mechanism for polymerization.

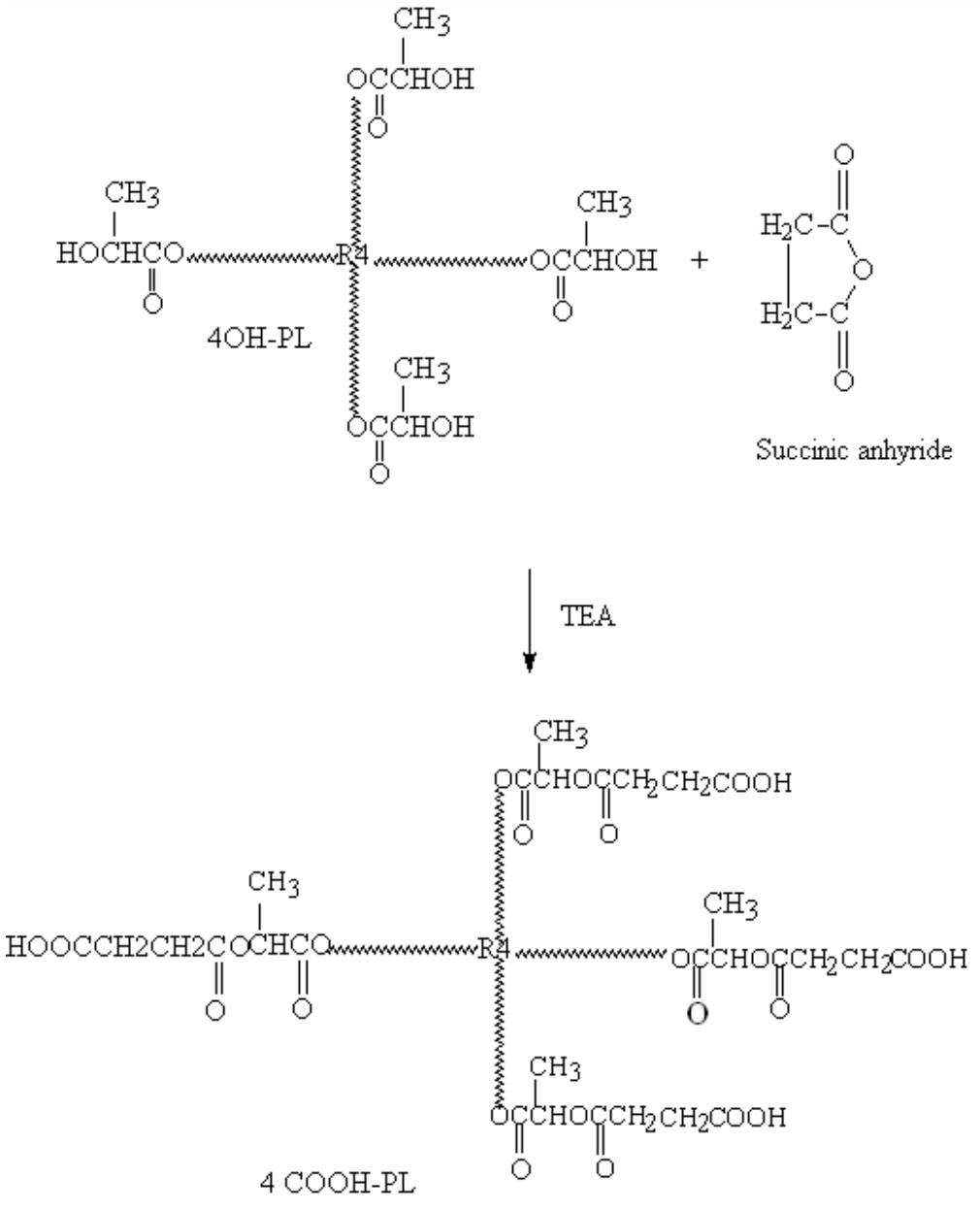

Figure 4.2: Acid modification reaction of 4-armed OH-PL to 4-armed COOH-PL.

COOH-PLs were prepared by reacting OH-PLs with succinic anhydride in the presence of TEA as a catalyst. All the reactions were carried out in 1,4-dioxane with continuous stirring for about 4 days in a water bath at 30^{o}C. The representative reaction scheme for 4-armed PL is shown in Figure 4.2.

The number- and weight-average molecular weights ($M_{n,GPC}$ and $M_{w,GPC}$) and molecular weight distribution of the resultant polymers were determined by GPC and are presented in Table 4.2. The theoretical number-average molecular weights (M_{theo}) were calculated using the $M_{n,GPC}$ of OH-PLs and succinic anhydride molecular weight.

Table 4.2: Molecular weights of COOH functional PLs determined by GPC and ^{1}H-NMR

	$M_{n,theo}$	**$M_{n,GPC}$**	**$M_{w,GPC}$**	**PD_{GPC}**	**Yield (%)**	**$M_{n,NMR}$**
1-armed COOH PL	**20,000**	**19,300**	**32,300**	**1.67**	**78**	**19,000**
2-armed COOH PL	**19,100**	**18,700**	**31,900**	**1.71**	**74**	**18,400**
3-armed COOH PL	**19,500**	**18,900**	**36,000**	**1.90**	**83**	**18,700**
4-armed COOH PL	**18,800**	**18,100**	**29,500**	**1.63**	**79**	**18,100**

The theoretical number-average molecular weight of COOH-PLs ($M_{n,theo}$) must be higher than the corresponding $M_{n,GPC}$ values of OH-PLs by the amount of succinic anhydride added to the chain ends. The $M_{n,NMR}$ of COOH-PLs found to be lower than the theoretical values probably because of the reaction medium. The reactions were carried out in the basic medium because of the catalyst, TEA. Although the reaction temperature was low, it is possible to have some decrease in molecular weight because of some degree of degradation during the reaction in the basic medium. Also, the lower yield percentage may indicate the possibility of some lost of the polymer during the precipitation and cleaning processes.

4.2. Characterization by ^{1}H-NMR

4.2.1. ^{1}H-NMR Characteristics of OH Functional Poly(L-lactide)s

The linear and multi-armed OH-PLs were analyzed for end-groups with a Bruker 250 MHz ^{1}H-NMR spectrometer in deuterated chloroform ($CDCl_3$). The ^{1}H-NMR spectrum of 1 OH-PL is shown in Figure 4.3 with the structure of the polymer. The assignments of the peaks are as follow:

δ=5.18 ppm {nH,q,[OCO-(CH)OCO]}; δ=4.38 ppm {1H,q,[OCO(CH)OH]}; δ=4.17 ppm {2H,t,[C(CH_2)OCO)]}, δ=1.59 ppm {3nH, d, (CH_3)}].

The characteristics of 1 OH-PL are given in Table 4.3. The number average molecular weight ($M_{n,NMR}$, Table 4.1) was calculated from the integral value ratios of the HCO methine proton of the repeating unit (*a*) at δ = 5.18 ppm and the HCOH methine proton of the end-group (*b*) at δ = 4.38 ppm (Table 4.3) in the ^{1}H-NMR spectrum of the 1 OH-PL. The $M_{n,NMR}$ value was calculated as 19,500 Da from the degree of polymerization (number of repeating units per terminal OH, *a*/*b* = 268) and the molecular weight of dodecanol. The integral ratio of methyl protons doublet signal (*d*) and the methine proton quartet (*a*) of the repeat unit was equal to 3:1. The integral ratio of methylene protons triplet signal (*c*) and the methine proton quartet (*b*) of the end-group was equal to 2 : 1 which indicated that there is one OH group per dodecanol molecule.

The ^{1}H-NMR spectrum of 2 OH-PL is shown in Figure 4.4 with the structure of the polymer. The assignments of the peaks are the same as 1 OH-PL except for integral values of the peaks (a) and (d).

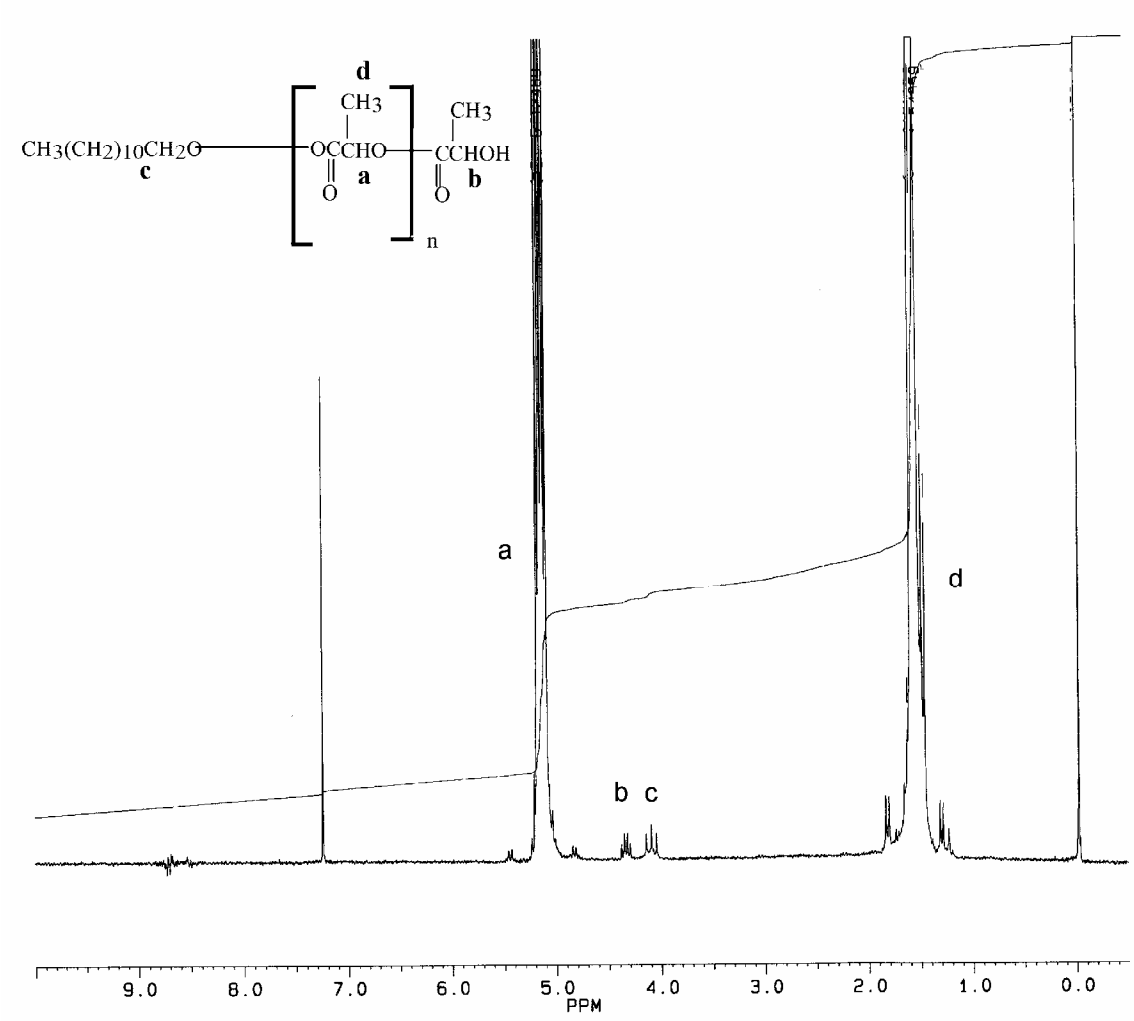

Figure 4.3: ^{1}H-NMR Spectrum of 1-armed OH-PL.

Table 4.3: ^{1}H-NMR Characteristics of 1-armed OH-PL.

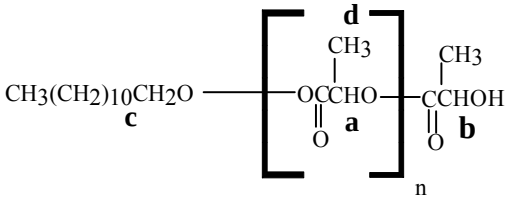

	δ (PPM)	Number of H	Number of Peaks	Integral
a	5.18	nH	quartet	75.20
b	4.38	1H	quartet	0.28
c	4.17	2H	triplet	0.56
d	1.59	3nH	doublet	225.50

The number average molecular weight ($M_{n,NMR}$, Table 4.1) of 2 OH-PL polymer was calculated from the integral value ratios of the HCO methine proton of the repeating unit (*a*) at δ = 5.18 ppm and the HCOH methine proton of the end-group (*b*) at δ = 4.38 ppm (Table 4.4). The $M_{n,NMR}$ value was calculated as 18,300 Da from the degree of polymerization (*a*/*b* = 127) and the molecular weight of ethylene glycol. In this calculation the degree of polymerization was multiplied by two since the polymer had two arms and *a*/*b* is the number of repeating units per terminal OH group. The integral ratio of methyl protons doublet signal (*d*) and the methine proton quartet (*a*) calculated as 3:1, which is expected from the repeat unit structure. The integral ratio of methylene protons triplet signal (*c*) and the methine proton quartet (*b*) of the end-group was equal to 2:1 which indicated that there is one OH group per OCH_2 in ethylene glycol molecule, or two OH groups per ethylene glycol molecule.

The ^{1}H-NMR spectrum of 3 OH-PL is shown in Figure 4.5 with the structure of the polymer. The assignments of the peaks are the same as 1 and 2 OH-PLs except for the doublet peak at δ = 4.17 ppm for this polymer is from OCH_2 groups in trimethylolpropane.

The number average molecular weight ($M_{n,NMR}$, Table 4.1) was calculated from the integral value ratios of the HCO methine proton of the repeating unit (*a*) and the HCOH methine proton of the end-group (*b*) (Table 4.5) in the ^{1}H-NMR spectrum of the 3 OH-PL. The $M_{n,NMR}$ value was calculated as 18,900 Da from the degree of polymerization (*a*/*b* = 87) and the molecular weight of trimethylolpropane. In this calculation the degree of polymerization was multiplied by three since the polymer had three arms and *a*/*b* is the number of repeating units per terminal OH group. As expected from the repeat unit structure, the integral ratio of methyl protons doublet signal (*d*) and the methine proton quartet (*a*) was 3:1. The integral ratio of methylene protons doublet signal (*c*) and the methine proton quartet (*b*) of the repeat unit was equal to 2:1 which indicated that there is one OH group per OCH_2 in trimethylolpropane molecule, or three OH groups per trimethylolpropane molecule.

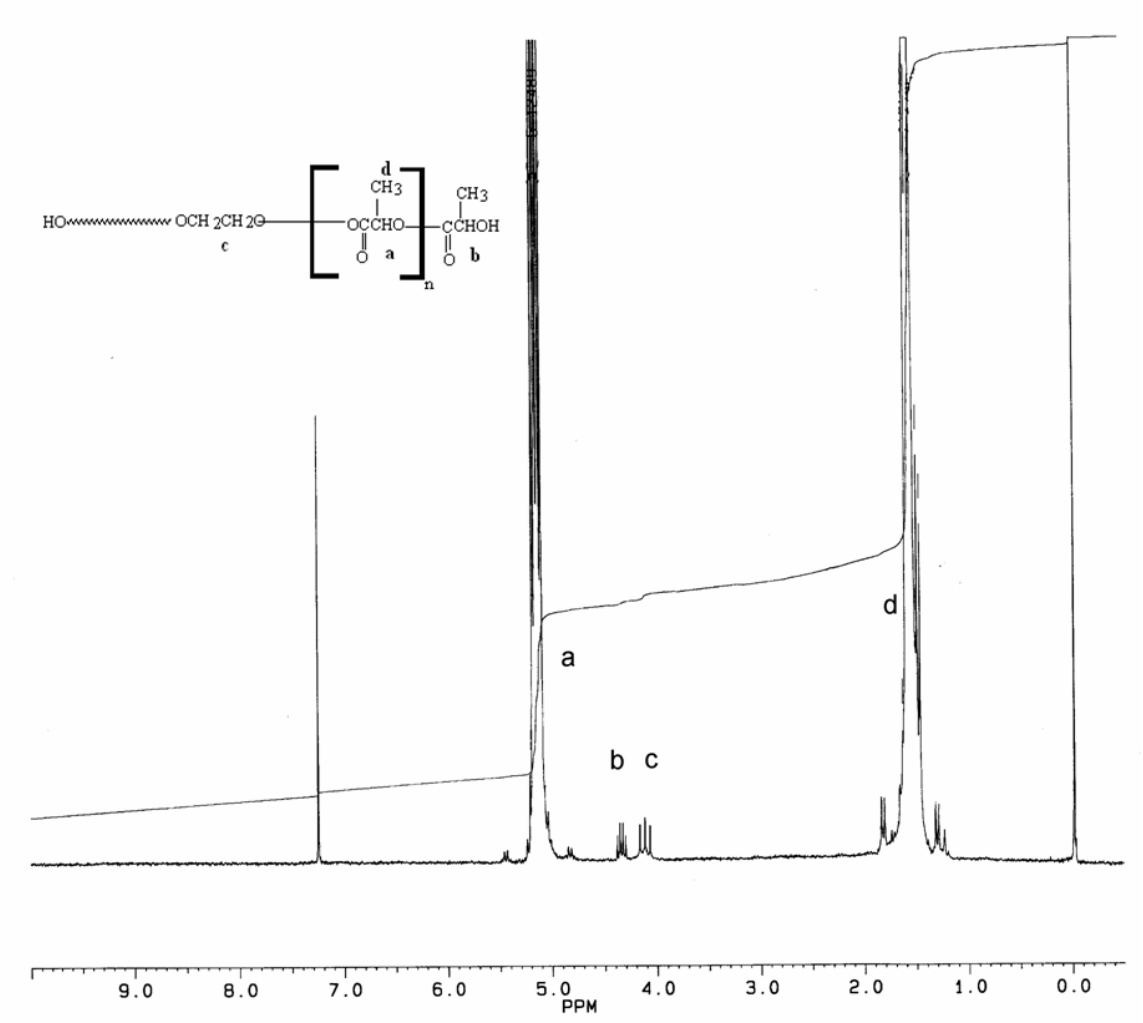

Figure 4.4: ^{1}H-NMR Spectrum of 2-armed OH-PL.

Table 4.4: ^{1}H-NMR Characteristics of 2-armed OH-PL.

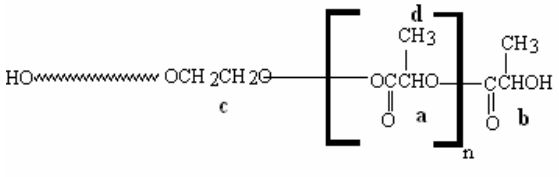

	δ (PPM)	Number of H	Number Of Peaks	Integral
a	5.18	nH	Quartet	36.77
b	4.38	2H	Quartet	0.29
c	4.17	4H	Triplet	0.58
d	1.59	3nH	Doublet	110.31

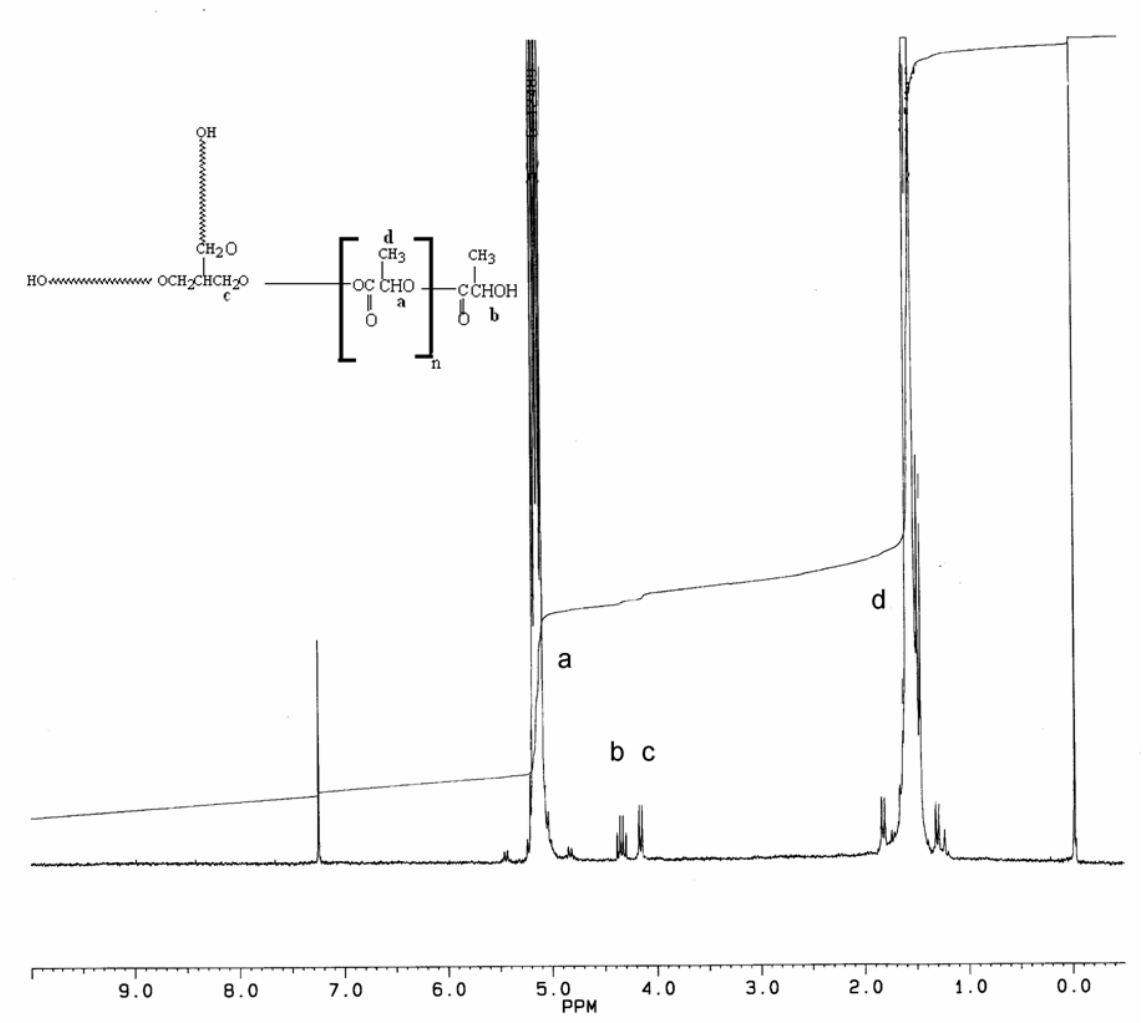

Figure 4.5: ^{1}H-NMR Spectrum of 3-armed OH-PL.

Table 4.5: ^{1}H-NMR Characteristics of 3-armed OH-PL.

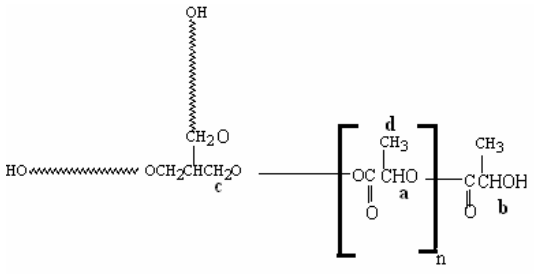

	δ (PPM)	Number of H	Number Of Peaks	Integral
a	5.18	nH	quartet	27.79
b	4.38	3H	quartet	0.32
c	4.17	6H	dublet	0.64
d	1.59	3nH	doublet	83.37

The ^{1}H-NMR spectrum of 4 OH-PL is shown in Figure 4.6 with the structure of the polymer. The assignments of the peaks are nearly the same as 1, 2 and 3 OH-PLs. the only difference is the singlet peak *(c)* at δ = 4.17 ppm for this polymer is from OCH_2 groups in pentaerythritol.

The characteristics of 4 OH-PL are given in Table 4.6. The number average molecular weight ($M_{n,NMR}$, Table 4.1) of this polymer was calculated from the integral value ratios of the HCO methine proton of the repeating unit (*a*) and the HCOH methine proton of the end-group (*b*) (Table 4.6). The $M_{n,NMR}$ value was calculated as 18,100 Da from the degree of polymerization (*a*/*b* = 62) and the molecular weight of pentaerythritol. In this calculation the degree of polymerization was multiplied by four since the polymer had four arms and *a*/*b* is the number of repeating units per terminal OH group. The integral ratio of methyl protons doublet signal (*d*) and the methine proton quartet (*a*) of the repeat unit was equal to 3:1. The integral ratio of methylene protons doublet signal (*c*) and the methine proton quartet (*b*) of the repeat unit was equal to 2:1 which indicated that there is one OH group per OCH_2 in pentaerythritol molecule, or four OH groups per pentaerythritol molecule.

Besides the ^{1}H-NMR spectra of linear and multi-armed OH PLs identified the end-groups but also proved the structure of the multi-armed OH Pls which have more than one end-group on each polymer molecule. For example, in a previous article, Lee et al. [11] carried out a proton exchange experiment and a model reaction between lactide and pentaerythritol for the assignment of the ^{1}H-NMR peaks. They reported a ^{1}H-NMR spectrum similar to Figure 4.6 for the four-armed poly(L-lactide). They found that the peaks at δ = 5.18, 4.38, and 1.59 ppm should be assigned to the methine proton resonance of the lactate, methine proton resonance at the end of the chain, and methyl protons on the lactate units, respectively. From their experiments, they have concluded that pentaerythritol methylene protons exhibited two peaks; the one attached to lactide was observed at δ = 4.17 and the one to unreacted pentaerythritol was observed at δ = 3.5 ppm. As can be seen in Figure 4.6, there is no signal at δ = 3.5 ppm, implying that all hydroxyl groups are reacted with lactide, resulting in a star-shaped structure.

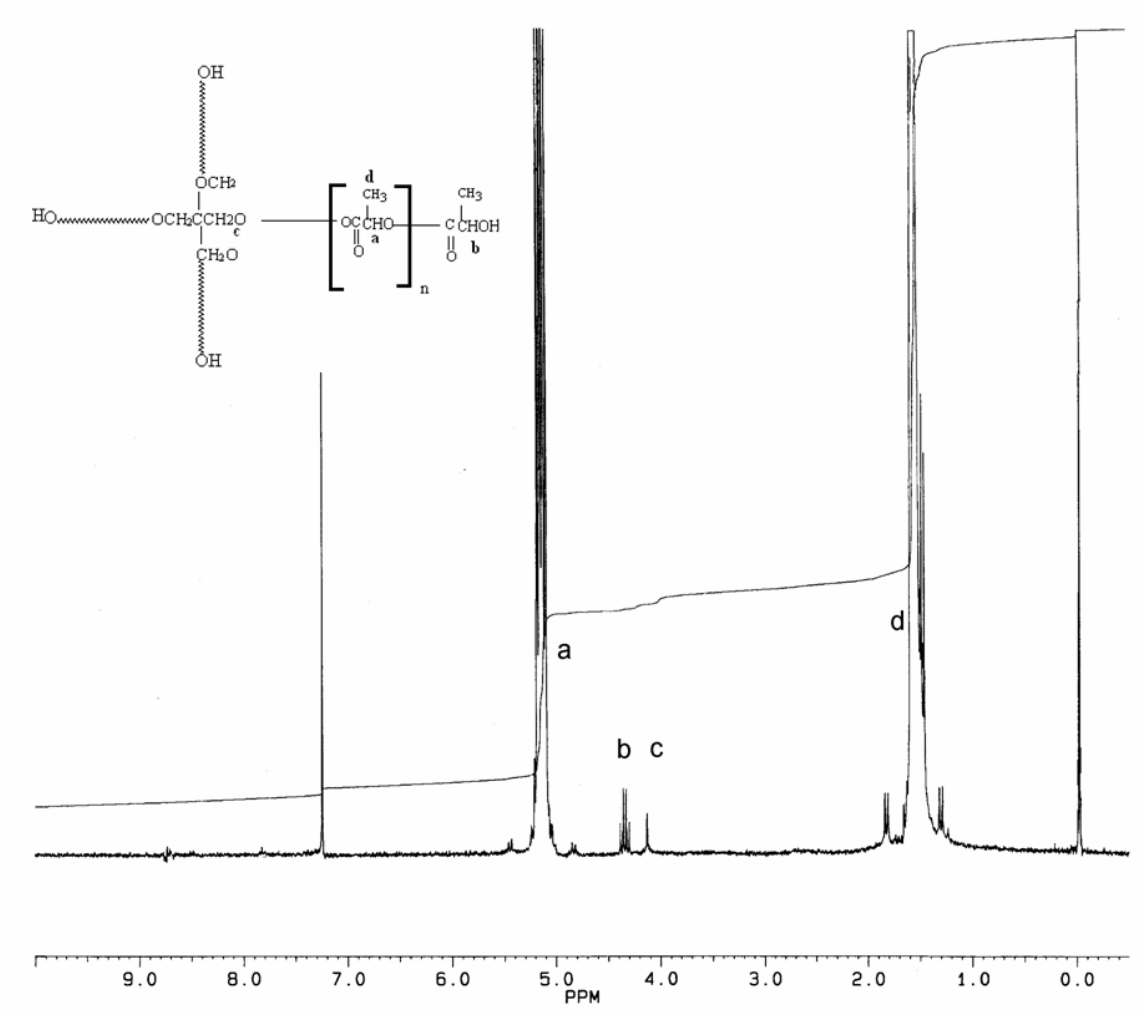

Figure 4.6: [1]H-NMR Spectrum of 4-armed OH-PL.

Table 4.6: [1]H-NMR Characteristics of 4-armed OH-PL.

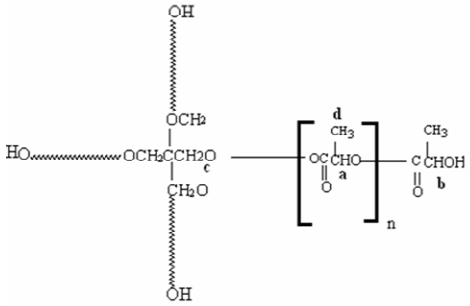

	δ (PPM)	Number of H	Number of Peaks	Integral
a	5.18	nH	quartet	21.18
b	4.38	4H	quartet	0.34
c	4.17	8H	singlet	0.68
d	1.59	3nH	doublet	63.50

In our study with the Sn-oct/pentaerythritol system, there is a theoretical possibility that the polymerization does not proceed via a pentaerythritol initiated mechanism but via Sn-oct, resulting in a linear polymer structure. However, the star-shaped structure of PL was deduced from the integration ratios of pentaerythritol methylene proton peak and the terminal methine peak which is 2:1, and the absence of δ = 3.5 ppm signal in its ^{1}H-NMR spectrum.

4.2.2. ^{1}H-NMR Characteristics of COOH Functional Poly(L-lactide)s

The ^{1}H-NMR spectra of linear and multi-armed COOH functional poly(L-lactide)s are given in Figures 4.7 – 4.10. In these spectra, the resonance peaks of methine protons (*b*) which were bonded to the hydroxyl end-group at the end of the chain (δ = 4.38 ppm) disappeared. On the other hand, new resonance peaks appeared at δ = 2.68 ppm which can be assigned for the methylene protons (*e*) (OCH_2CH_2COOH) from the reacted succinic anhydride. The disappearance of δ = 4.38 ppm peaks and appearance of δ = 2.68 ppm peaks indicated the reaction between OH end-groups in OH PLs and succinic anhydride carried out almost completely.

The assignments of the peaks from the ^{1}H-NMR spectrum of 1 COOH PL (Figure 4.7) are as follow:

δ = 5.18 ppm {nH,q,[OCO-(CH)OCO]}; δ = 2.68 ppm {4H, t ,[OCO(CH_2CH_2)-COOH]}; δ = 4.17 ppm {2H, t, [C(CH_2)OCO)]}; δ = 1.59 ppm {3nH, d, (CH_3)}].

and the characteristics are given in Table 4.7. The number average molecular weight ($M_{n,NMR}$, Table 4.2) was calculated from the integral value ratios of the HCO methine proton of the repeating unit (*a*) at δ = 5.18 ppm and the methylene protons (OCH_2CH_2COOH) of the end-group (*e*) at δ = 2.68 ppm (Table 4.7). The $M_{n,NMR}$ value was calculated as 19,000 Da from the degree of polymerization (number of repeating units per terminal COOH, *a*/(*e/4)* = 262) and the molecular weight of dodecanol. In this calculation, the integral value of methylene peaks was divided by four because of the four protons in

(OCH_2CH_2COOH) and one methine proton in the repeating unit. The integral ratio of methyl protons doublet signal (*d*) and the methine proton quartet (*a*) of the repeat unit was equal to 3:1. The ratio of methylene protons at the end-group (*e*) to methylene protons in dodecanol (*c*) was calculated as 2:1, which indicated that there is one COOH group or dodecanol molecule.

The ^{1}H-NMR spectrum of 2 COOH-PL and its characteristics are depicted in Figure 4.8 and Table 4.8, respectively, with the structure of the polymer. The assignments of the peaks are the same as 1 COOH-PL except the peak at δ = 4.17 ppm for this polymer is from OCH_2 group in ethylene glycol. The number average molecular weight ($M_{n,NMR}$, Table 4.2) was calculated from the integral value ratios of the HCO methine proton of the repeating unit (*a*) at δ = 5.18 ppm and the methylene protons of the end-group (*e*) at δ = 2.68 ppm (Table 4.6). The $M_{n,NMR}$ value was calculated as 18,300 Da from the degree of polymerization (*a*/(*e/4)* = 127) and the molecular weight of ethylene glycol. In this calculation the degree of polymerization was multiplied by two since the polymer had two arms and *a*/(*e/4)* is the number of repeating units per terminal COOH group. The integral ratio of methyl protons doublet signal (*d*) and the methine proton quartet (*a*) of the repeat unit was equal to 3:1, as expected. The integral ratio of methylene protons triplet signal (*e*) and the methylene protons triplet (*c*) of the end-group was equal to 2 : 1 which indicated that there are two COOH groups per ethylene glycol molecule.

The ^{1}H-NMR spectrum of 3 COOH-PL is shown in Figure 4.9 with the structure of the polymer. The assignments of the peaks are the same as 1 and 2 COOH-PLs except the doublet peak at δ = 4.17 ppm for this polymer is from OCH_2 group in trimethylolpropane. The number average molecular weight ($M_{n,NMR}$, Table 4.2) was calculated from the integral value ratios of the HCO methine proton of the repeating unit (*a*) and the (OCH_2CH_2COOH) methylene protons of the end-group (*e*) (Table 4.9). The $M_{n,NMR}$ value was calculated as 18,900 Da from the degree of polymerization (*a*/*(e/4)* = 86) and the molecular weight of trimethylolpropane. In this calculation the degree of polymerization was multiplied by three since the polymer had three arms and *a*/*(e/4)* is the number of repeating units per terminal COOH group. As expected, the integral ratio of methyl protons doublet signal (*d*)

and the methine proton quartet (*a*) of the repeat unit was calculated as 3:1. The integral ratio of methylene protons triplet signal (*e*) and the methylene protons doublet (*c*) of the trimethylolpropane was equal to 2:1 which indicated that there is one COOH group per OCH_2 in trimethylolpropane molecule, or three COOH groups per trimethylolpropane molecule.

The ^{1}H-NMR spectrum of 4 COOH-PL is shown in Figure 4.10 with the structure of the polymer. The assignments of the peaks are the same as 1, 2 and 3 COOH-PLs except the singlet peak at $\delta = 4.17$ ppm for this polymer is from OCH_2 group in pentaerythritol.

The characteristics of 4 COOH-PL are given in Table 4.10. The number average molecular weight ($M_{n,NMR}$, Table 4.2) was calculated from the integral value ratios of the HCO methine proton of the repeating unit (*a*) and the (OCH_2CH_2COOH) methylene protons of the end-group (*e*) (Table 4.10). The $M_{n,NMR}$ value was calculated as 18,100 Da from the degree of polymerization (*a*/*(e/4)* = 63) and the molecular weight of pentaerythritol. In this calculation the degree of polymerization was multiplied by four since the polymer had four arms and *a*/*(e/4)* is the number of repeating units per terminal COOH group. The integral ratio of methyl protons doublet signal (*d*) and the methine proton quartet (*a*) of the repeat unit was calculated to be 3:1. The integral ratio of methylene protons triplet signal (*e*) and the methylenene proton singlet (*c*) of the pentaerythritol was equal to 2 : 1 which indicated that there is one COOH group per OCH_2 in pentaerythritol molecule, or four COOH groups per pentaerythritol molecule.

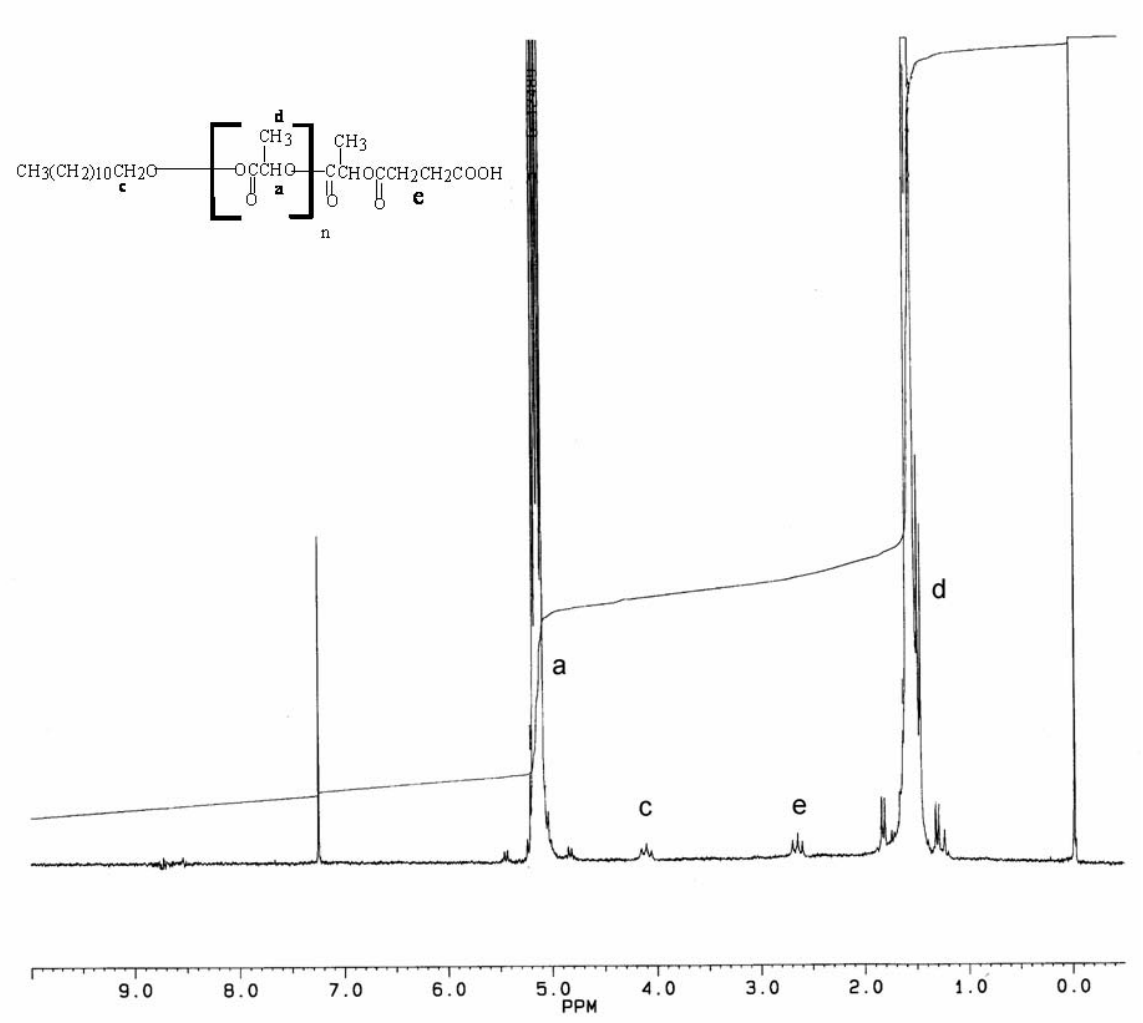

Figure 4.7: ^{1}H-NMR Spectrum of 1-armed COOH-PL.

Table 4.7: ^{1}H-NMR Characteristics of 1-armed COOH-PL

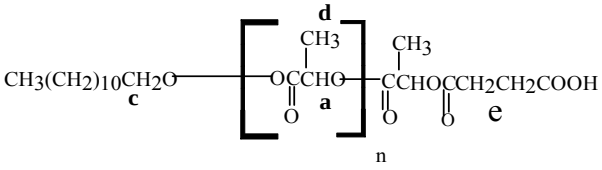

	δ (PPM)	Number of H	Number Of Peaks	Integral
a	5.18	nH	quartet	71.94
c	4.17	2H	triplet	0.54
e	2.68	4H	triplet	1.10
d	1.59	3nH	doublet	215.80

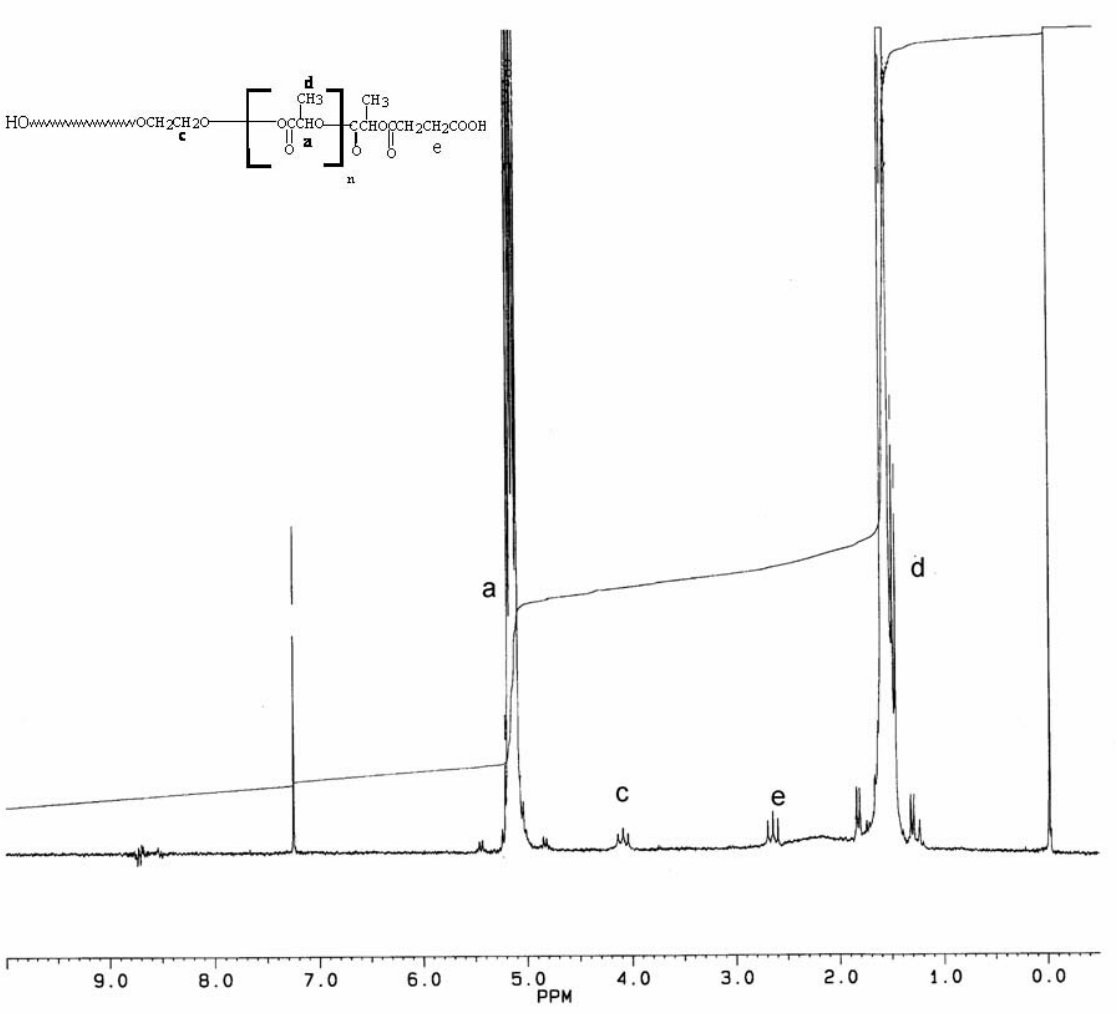

Figure 4.8: ^{1}H-NMR Spectrum of 2-armed COOH-PL.

Table 4.8: ^{1}H-NMR Characteristics of 2-armed COOH-PL.

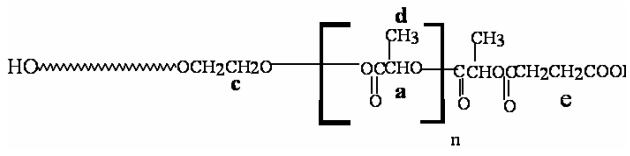

	δ (PPM)	Number of H	Number of Peaks	Integral
a	5.18	nH	quartet	36.30
c	4.17	4H	triplet	0.57
e	2.68	8H	triplet	1.14
d	1.59	3nH	doublet	108.92

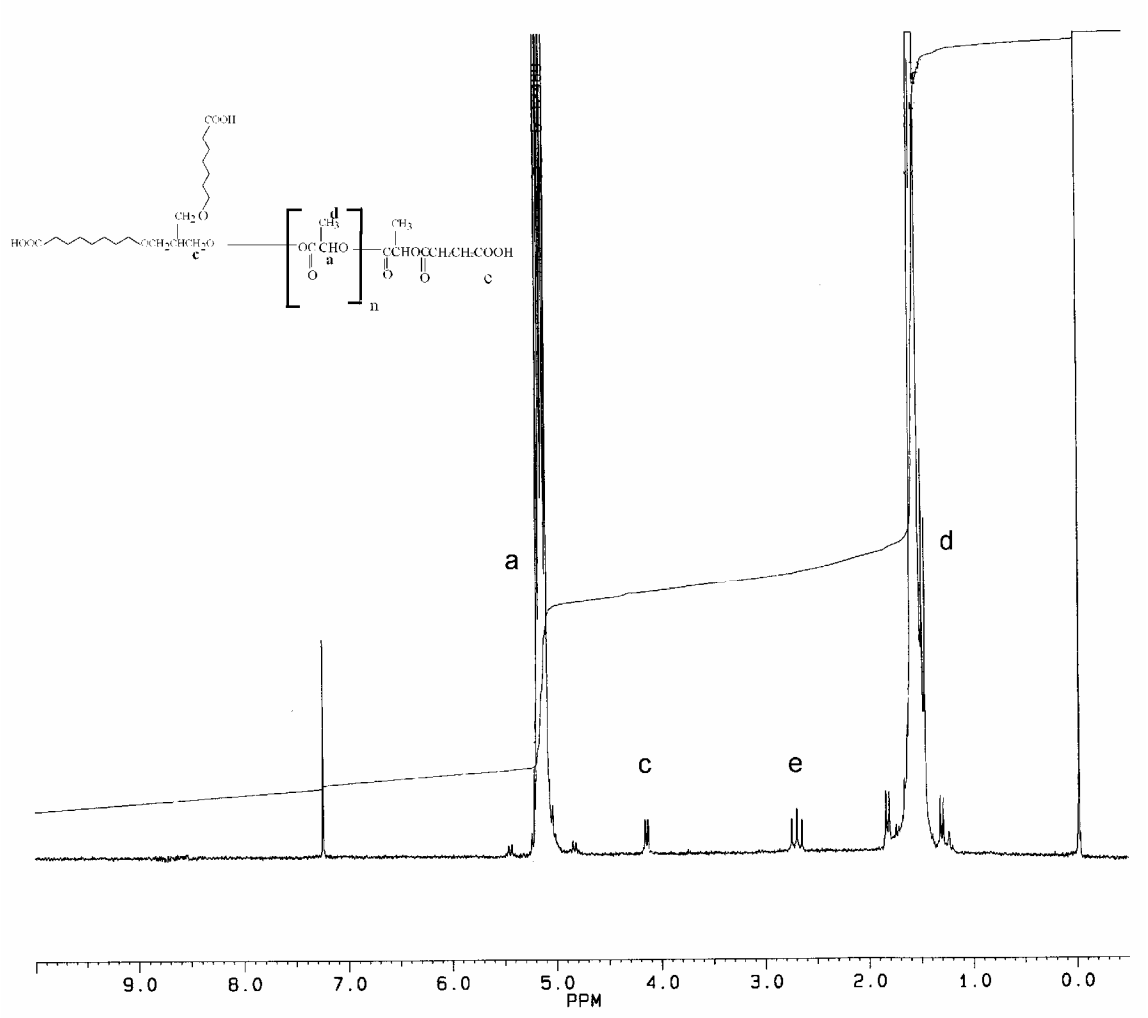

Figure 4.9: ^{1}H-NMR Spectrum of 3-armed COOH-PL.

Table 4.9: ^{1}H-NMR Characteristics of 3-armed COOH-PL.

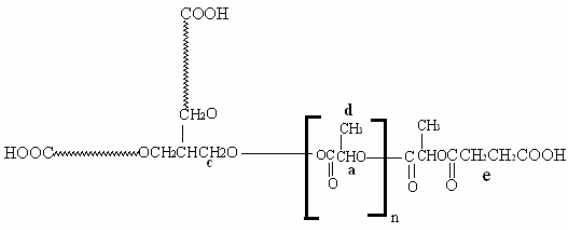

	δ (PPM)	Number of H	Number of Peaks	Integral
a	5.18	nH	quartet	26.63
c	4.17	6H	dublet	0.62
e	2.68	12H	triplet	1.22
d	1.59	3nH	doublet	79.90

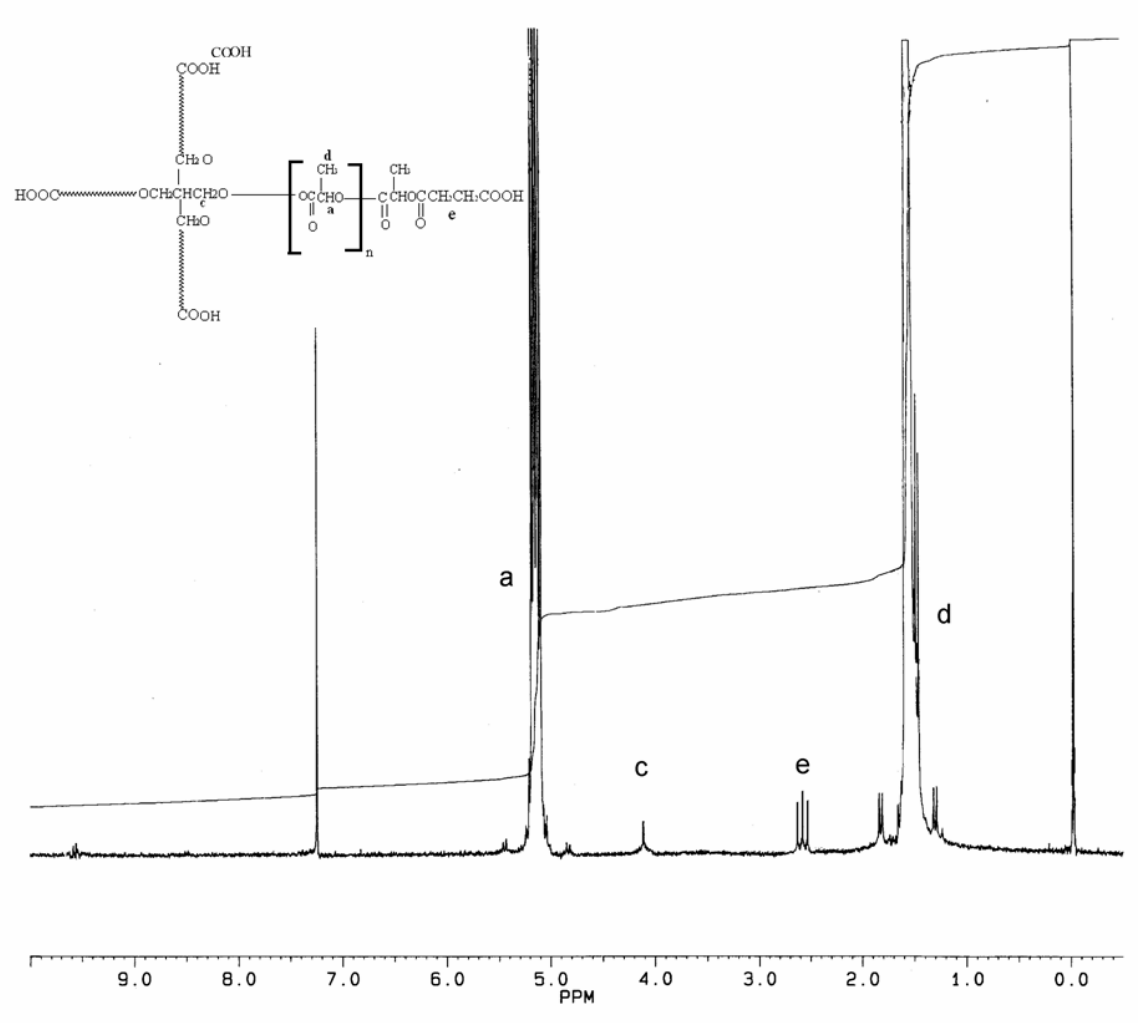

Figure 4.10: ^{1}H-NMR Spectrum of 4-armed COOH-PL.

Table 4.10: ^{1}H-NMR Characteristics of 4-armed COOH-PL.

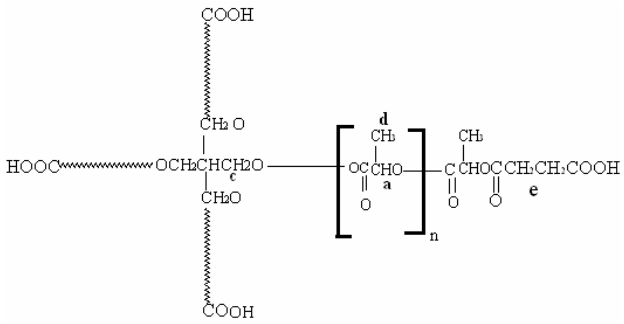

	δ (PPM)	Number of H	Number Of Peaks	Integral
a	5.18	nH	quartet	19.59
c	4.17	8H	singlet	0.63
e	2.68	16H	triplet	1.26
d	1.59	3nH	doublet	58.77

4.3. Thermal Degradation

The thermal degradation behavior of OH and COOH functional, linear and multi-armed PLs were explored by dynamic thermogravimetry. The thermogravimetric data for each OH-PLs and COOH-PLs sample were collected under steady flow of nitrogen from room temperature to 450 ^{o}C at various heating rates (10 to 50 K/min) to study their thermal degradation kinetics. The heating rate range of 10-50 K/min was selected to prevent side reactions at higher temperatures. At slower heating rate (<10 K/min) the residence time of the sample at the higher temperatures will be longer which may cause undesirable degradation or side reactions. Also, nitrogen was chosen as the carrier gas and degradation medium, rather than oxygen or air, to prevent possible oxidation reactions which may take place at higher temperatures.

4.3.1. Thermal Degradation of OH-PLs

To analyze the effect of the end-group concentration in the thermal degradation behavior of linear and multi-armed OH-PLs, the thermal degradation of these polymers was studied by measuring the weight loss of the powder samples as a function of linear increase in temperature using TGA. The TGA thermograms of dynamic degradation of 1-armed OH-PL, 2-armed OH-PL, 3-armed OH-PL and 4-armed OH-PL are shown in Figures 4.11-4.14. In these figures, the remaining weight percents were plotted against the temperature in ^{o}C.

In these figures, the remaining weight percents smoothly decreased to reach almost complete degradation. About 95 percent of weight loss took place at a 70^{o}C temperature range regardless of the heating rates and the number of end-groups. In each figure, the thermograms shifted to higher temperatures upon increasing the heating rates. In other words, thermal degradation started at higher temperatures with increasing the heating rate. For example, increasing the heating rate from 10 to 50 K/min for 1-armed OH-PL, 2-armed OH-PL, 3-armed OH-PL and 4-armed OH-PL, the degradation temperature increases in the

range of 55-60^{o}C at 50 percent degradation. This phenomenon is a typical and related to the shorter residence time of the sample during higher heating rates.

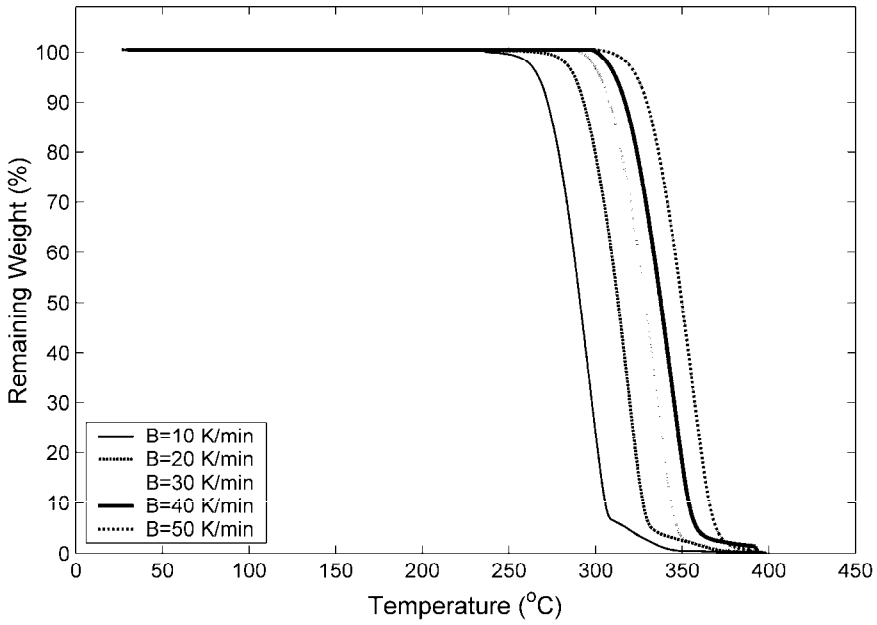

Figure 4.11: TGA Thermograms of 1-armed OH-PL at heating rates of 10, 20, 30, 40, and 50 K/min.

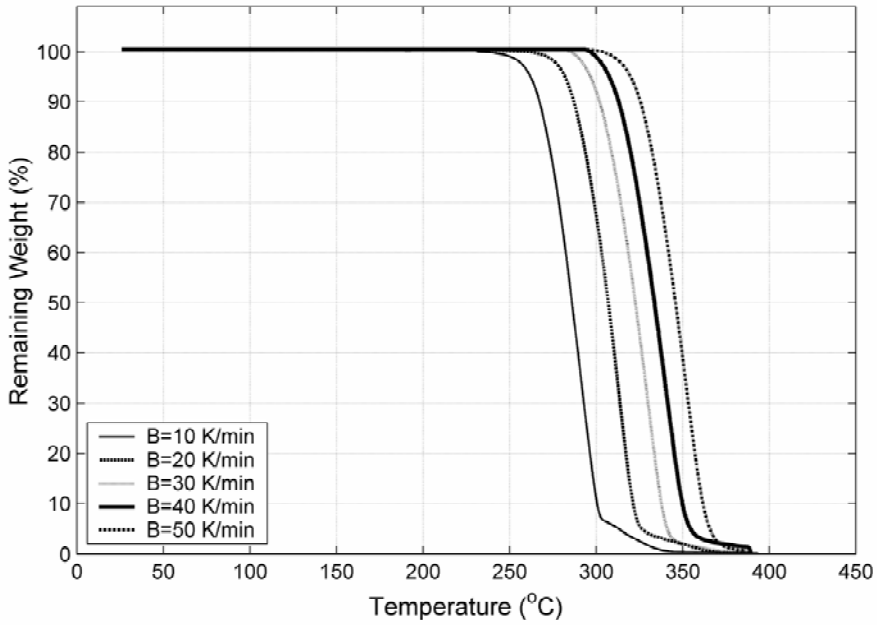

Figure 4.12: TGA Thermograms of 2-armed OH-PL at heating rates of 10, 20, 30, 40, and 50 K/min.

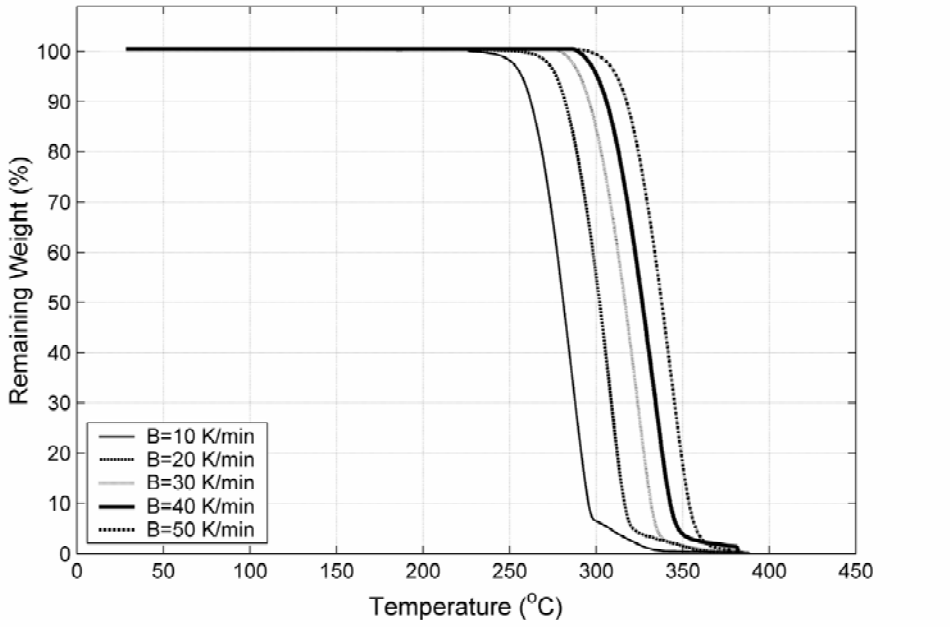

Figure 4.13: TGA Thermograms of 3-armed OH-PL at heating rates of 10, 20, 30, 40, and 50 K/min.

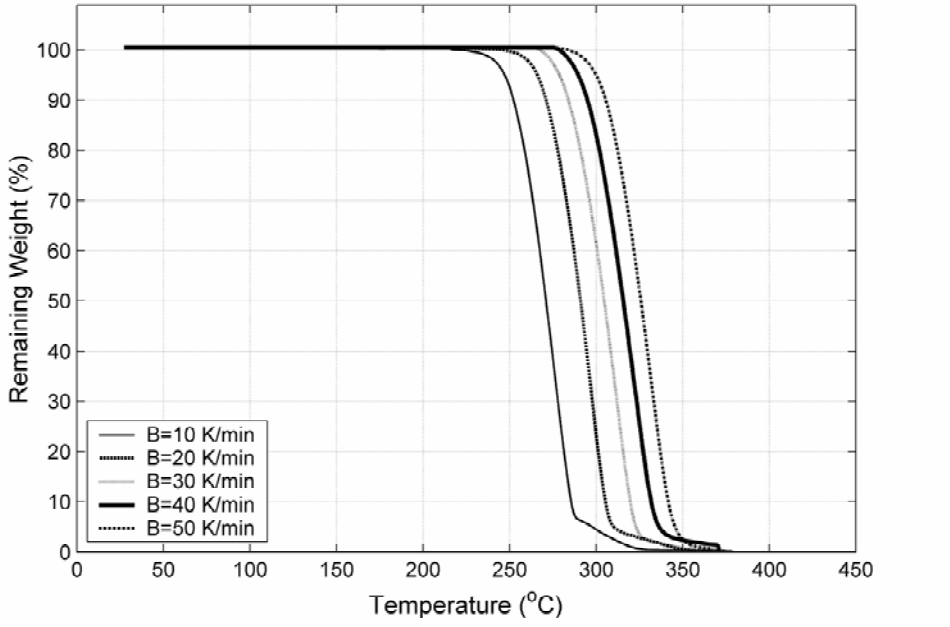

Figure 4.14: TGA Thermograms of 4-armed OH-PL at heating rates of 10, 20, 30, 40, and 50 K/min.

To see the effect of end-group concentration, the thermogravimetric data taken at the same heating rate (10 K/min) were plotted and is shown in Figure 4.15. In this figure, the thermal stability of OH-PLs decreased with an increasing end-group concentration. The linear OH-PL has the highest thermal stability whereas star-shaped OH-PL has the least. Since the OH-PLs have about the same number average molecular weight, the difference in thermal stability can be attributed to the end-group concentration; this difference in thermal stability is expected, because the 4-armed OH-PL degraded from four ends and 1-armed OH-PL degraded from only one end.

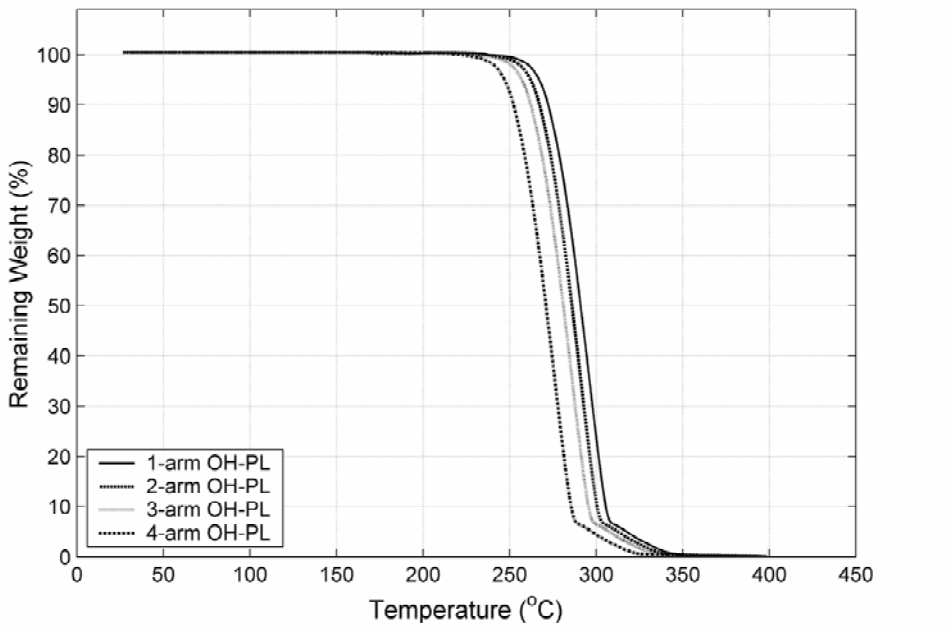

Figure 4.15: TGA Thermograms of 1-armed, 2-armed, 3-armed and 4-armed OH-PLs at heating rate of 10 K/min.

The effect of molecular weight on the thermal degradation behavior of OH-PLs was reported previously [17]. The degradation temperature increases as the molecular weight is increasing up to about 50,000 Da and then remains about the same [17]. In our study, the molecular weight of each armed is changing from about 20,000 to 9,000, 6,400 and 4,600 Da as the number of end-groups is increasing from 1 to 4 per polymer molecule. Decreasing molecular weight of each arm causes the degradation rate to increase. Therefore, the degradation of multi-armed OH-PLs at lower temperatures is expected.

The activation energies for the thermal degradation of OH-PLs were calculated using Ozawa's [86] and Reich's [87] approaches at various fractions of degradation (0.1-0.9). The fractions of degradation were calculated from the thermograms by

$$\alpha = (100 - \text{remaining weight percent}) / 100 \tag{4.1}$$

Ozawa [86] derived the following equation for thermal degradation of polymers

$$E = \frac{R \log B_2 / B_1}{0.457(1/T_1 - 1/T_2)} \tag{4.2}$$

For a given degradation fraction, α, the above equation can be rearranged and written as

$$\log B = -\frac{0.457E}{RT} \tag{4.3}$$

for the calculation of activation energy, E, in J/mol, for dynamic degradation. Here, R is the gas constant in J/K-mol, B is heating rate in K/min, and T is the temperature in K.

Therefore, the plot of log$B$ against the reciprocal absolute temperature for a given value of α, must be a straight line, the slope of which yields the activation energy. Almost linear parallel lines were obtained using least squares method; from which the activation energies were calculated and reported as E_a Ozawa. The log$B$ – 1/T plots for 1-armed OH-PL, 2-armed OH-PL, 3-armed OH-PL and 4-armed OH-PL are shown in Figures 4.16-4.19. Their calculated activation energies at various α values are tabulated in Tables 4.11-4.14.

Similarly, for calculation of the activation energy at a specific fraction of degradation, α, from the TGA data Reich [87] proposed the following equation:

$$E = \frac{R \ln[(B_2 / B_1)(T_1 / T_2)^2]}{1/T_1 - 1/T_2} \tag{4.4}$$

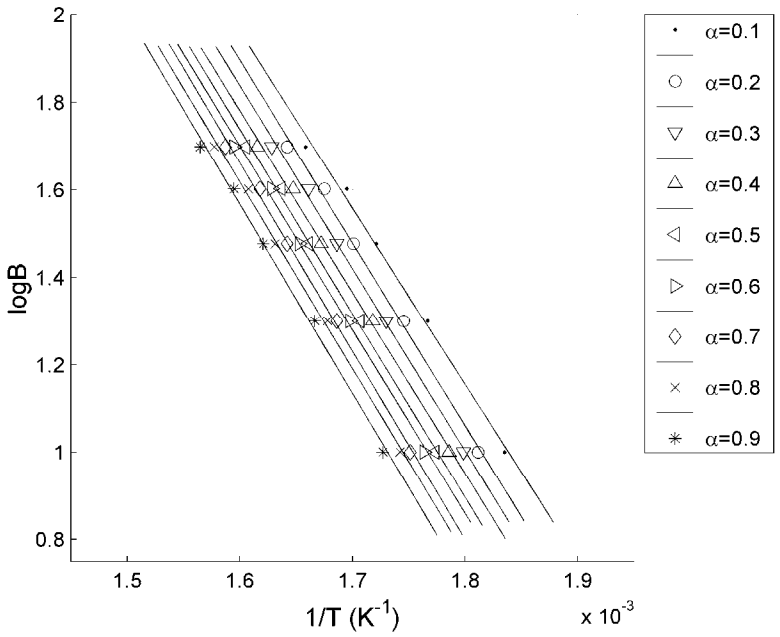

Figure 4.16: Ozawa plots of 1-armed OH-PL at varied fractions of degradation, α = 0.9 to 0.1

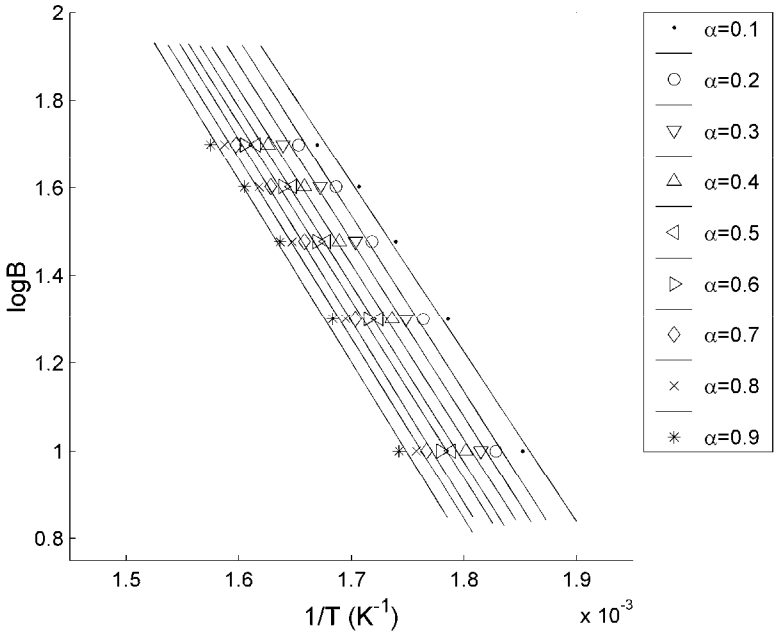

Figure 4.17: Ozawa plots of 2-armed OH-PL at varied fractions of degradation, α = 0.9 to 0.1

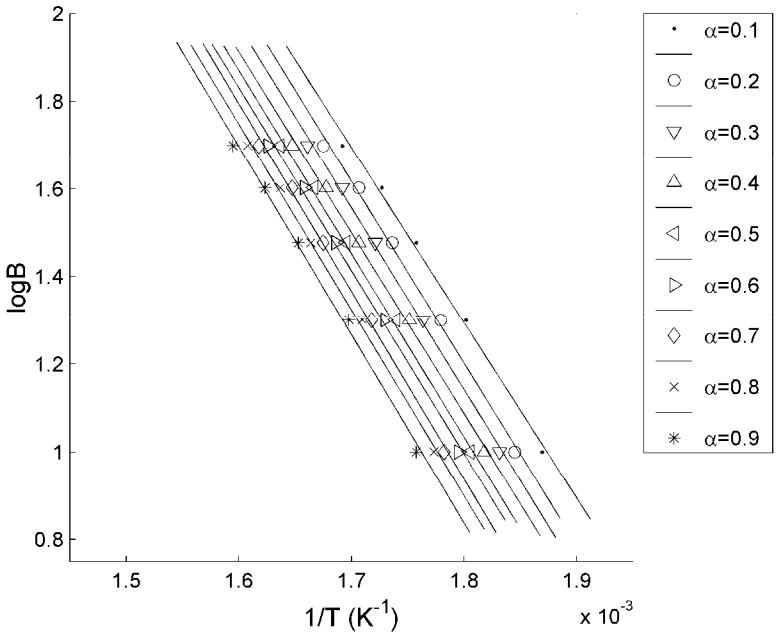

Figure 4.18: Ozawa plots of 3-armed OH-PL at varied fractions of degradation, $\alpha = 0.9$ to 0.1

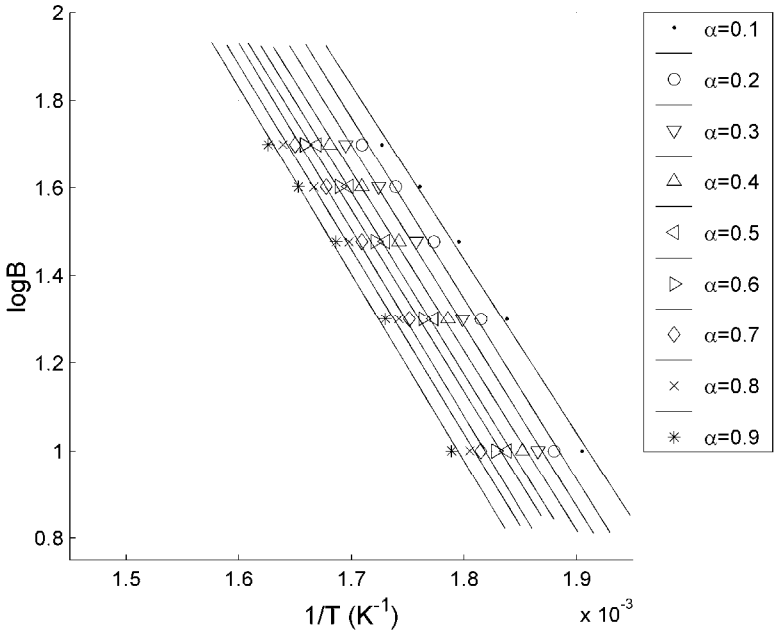

Figure 4.19: Ozawa plots of 4-armed OH-PL at varied fractions of degradation, $\alpha = 0.9$ to 0.1

Table 4.11: Calculated activation energies using Ozawa and Reich approaches for 1-armed OH-PL

B (^{o}C/min)	**10**	**20**	**30**	**40**	**50**		
α	**Temperature (^{o}C)**					**E_a Ozawa**	**E_a Reich**
0.1	272	293	308	317	330	73.3	67.7
0.2	279	300	315	324	336	76.1	70.4
0.3	283	305	320	329	341	76.0	70.3
0.4	287	309	325	334	346	75.6	69.8
0.5	291	313	329	338	350	76.6	70.8
0.6	294	316	332	341	354	76.5	70.6
0.7	298	320	336	345	357	78.4	72.6
0.8	301	323	340	349	361	77.7	71.7
0.9	306	327	344	354	366	78.7	72.7
Average E_a (kJ/mol)						76.5	70.7
Standard Deviation						±1.6	±1.5

Table 4.12: Calculated activation energies using Ozawa and Reich approaches for 2-armed OH-PL

B (^{o}C/min)	**10**	**20**	**30**	**40**	**50**		
α	**Temperature (^{o}C)**					**E_a Ozawa**	**E_a Reich**
0.1	267	287	302	313	326	72.8	67.3
0.2	274	294	309	320	332	75.6	70.1
0.3	278	299	314	325	337	75.6	70.0
0.4	282	303	319	330	342	75.1	69.4
0.5	286	307	323	334	346	76.1	70.5
0.6	289	310	326	337	350	76.0	70.3
0.7	293	314	330	341	353	78.0	72.3
0.8	296	317	334	345	357	77.2	71.4
0.9	301	321	338	350	362	78.2	72.4
Average E_a (kJ/mol)						76.1	70.4
Standard Deviation						±1.6	±1.6

Table 4.13: Calculated activation energies using Ozawa and Reich approaches for 3-armed OH-PL

B (^{o}C/min)	**10**	**20**	**30**	**40**	**50**		
α	**Temperature (^{o}C)**					**E_a Ozawa**	**E_a Reich**
0.1	262	282	296	306	318	72.3	66.9
0.2	269	289	303	313	324	75.1	69.7
0.3	273	294	308	318	329	75.0	69.6
0.4	277	298	313	323	334	74.6	69.0
0.5	281	302	317	327	338	75.6	70.1
0.6	284	305	320	330	342	75.5	70.0
0.7	288	309	324	334	345	77.5	71.9
0.8	291	312	328	338	349	76.7	71.1
0.9	296	316	332	343	354	77.6	71.9
Average E_a (kJ/mol)						75.5	70.0
Standard Deviation						±1.6	±1.6

Table 4.14: Calculated activation energies using Ozawa and Reich approaches for 4-armed OH-PL

B (°C/min)	**10**	**20**	**30**	**40**	**50**		
α	**Temperature (°C)**					**E_a Ozawa**	**E_a Reich**
0.1	252	271	284	295	306	70.5	64.7
0.2	259	278	291	302	312	73.1	67.4
0.3	263	283	296	307	317	73.1	67.3
0.4	267	287	301	312	322	72.8	66.9
0.5	271	291	305	316	326	73.8	67.8
0.6	274	294	308	319	330	73.7	67.7
0.7	278	298	312	323	333	75.5	69.6
0.8	281	301	316	327	337	74.9	68.8
0.9	286	305	320	332	342	75.7	69.7
Average E_a (kJ/mol)						73.7	67.8
Standard Deviation						±1.6	±1.5

which can be rewritten as

$$\ln\left(B/T^2\right) = -\frac{E}{RT} \tag{4.5}$$

Here, *B*, *T*, *E* and *R* have the same definitions and units as using Ozawa's approach.

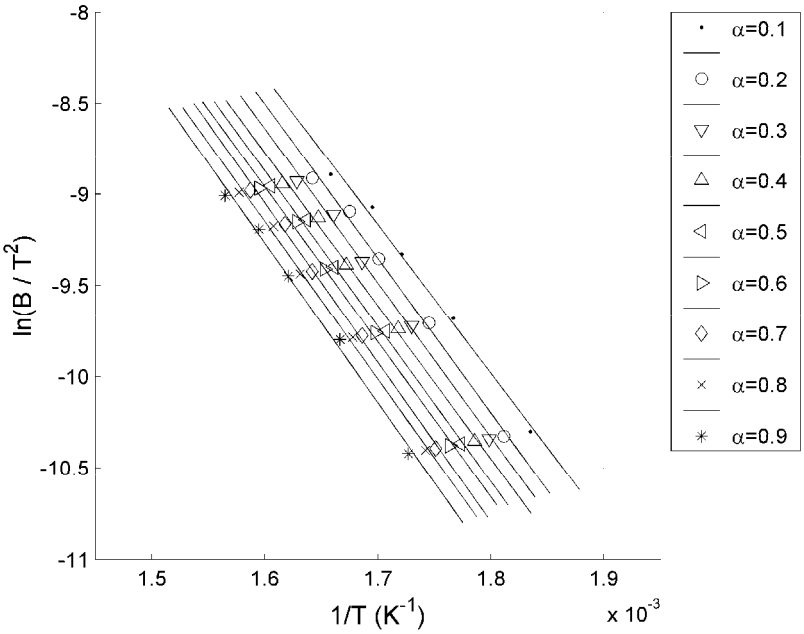

Figure 4.20: Reich plots of 1-armed OH-PL at varied fractions of degradation, $\alpha = 0.9$ to 0.1

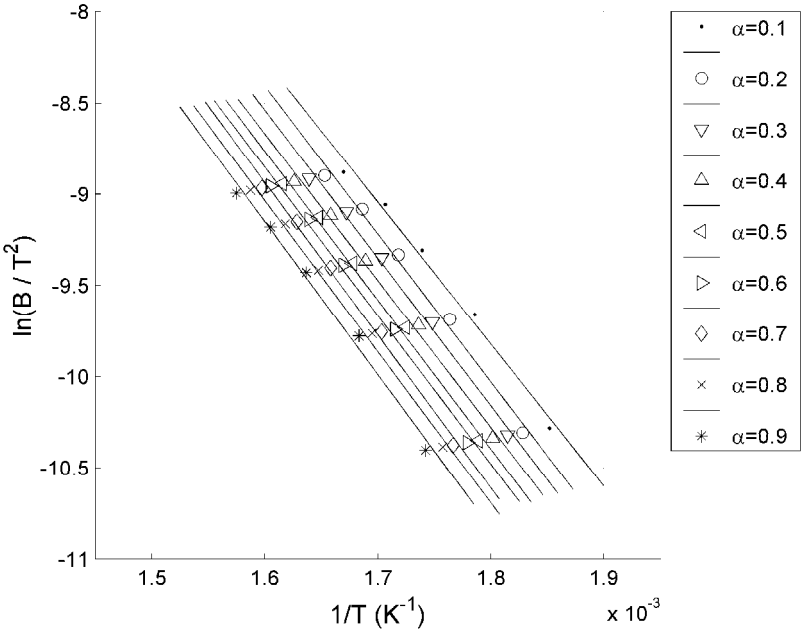

Figure 4.21: Reich plots of 2-armed OH-PL at varied fractions of degradation, $\alpha = 0.9$ to 0.1

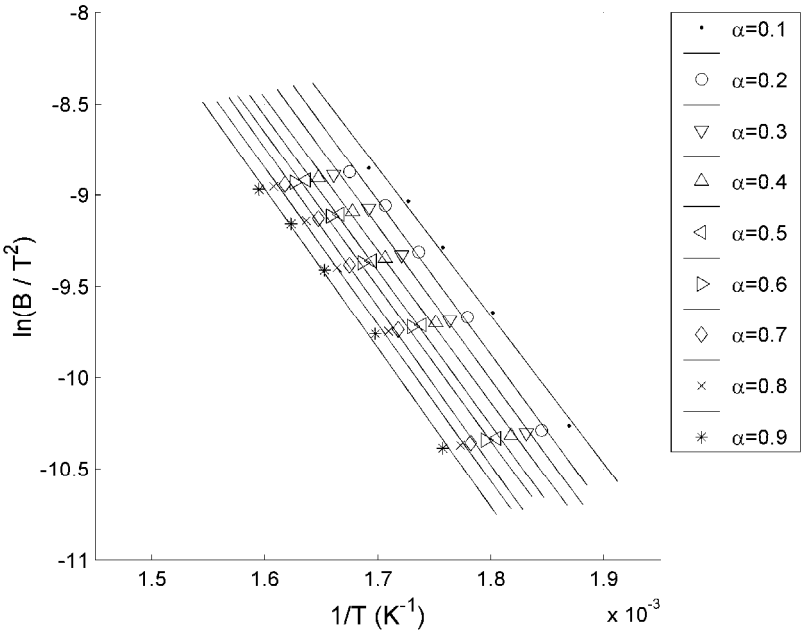

Figure 4.22: Reich plots of 3-armed OH-PL at varied fractions of degradation, $\alpha = 0.9$ to 0.1

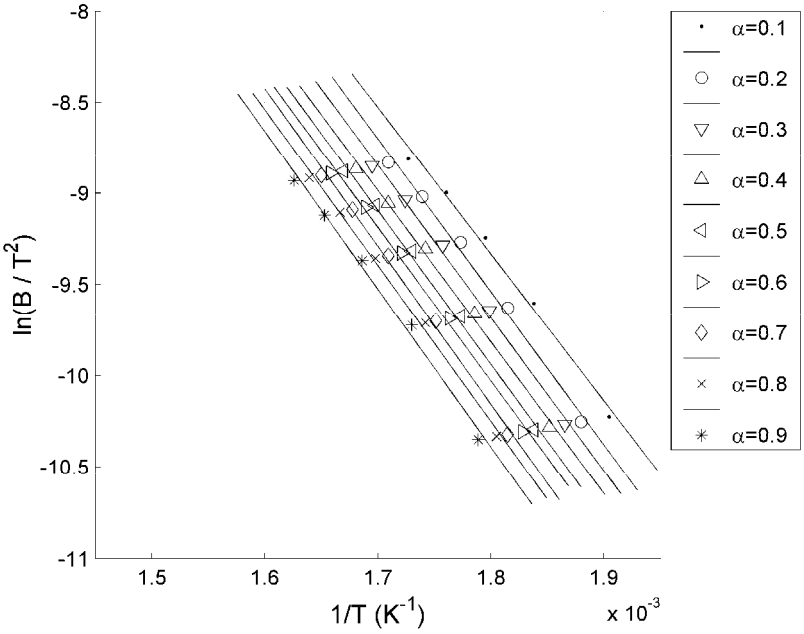

Figure 4.23: Reich plots of 4-armed OH-PL at varied fractions of degradation, α = 0.9 to 0.1

In Reich's, a plot of ln(B/T^2) against 1/T will give a straight line and the activation energy can be calculated from its slope. The ln(B/T^2) – 1/T plots for linear and multi-armed OH-PLs were plotted and are shown in Figures 4.10-4.23. Their calculated activation energies at various α values are tabulated in Tables 4.11-4.14 as E_a Reich.

The following points can be highlighted by examining the calculated activation energies using Ozawa's and Reich's approaches from Tables 4.11-4.14 for thermal degradation of linear and multi-armed OH-PLs at α values from 0.1 to 0.9.

In both approaches, the calculated activation energies decreased slightly as the end-group concentration increased. The effect of end-group concentration on degradation rate can also be seen in Figure 4.15. This slight difference in activation energy and rate of degradation may be explained by the average molecular weight of each arm. As mentioned previously, the average molecular weight per arm decreased from about 20,000 to 4,600 Da as the number of arms increased from 1 to 4. It was also mentioned that the degradation temperature increases as the molecular weight is increasing up to about 50,000 Da.

Therefore, it is expected that the thermal degradation rate increased as the end-group concentration increased at about the same molecular weight.

Secondly, the calculated activation energies by both of the approaches increased slightly as the α increased from 0.1 to 0.9. The difference is so small that no change occurs in the thermal degradation mechanism of the OH-PLs can be assumed with degree of degradation.

Thirdly, the calculated average activation energies by Reich's approach are about 6 kJ/mol less than the average activation energies calculated by Ozawa's approach which may be because of the assumptions done during the derivation of the equations used for calculation.

4.3.2. Thermal Degradation of COOH-PLs

The effect of COOH end-groups on thermal degradation behavior of PLs was also explored by dynamic thermogravimetry. The weight loss of linear and multi-armed COOH-PLs powder samples were measured as a function of linear increase in temperature using TGA. The TGA thermograms of dynamic degradation of 1-armed COOH-PL, 2-armed COOH-PL, 3-armed COOH-PL, and 4-armed COOH-PL are depicted in Figures 4.24-4.27 for the heating rate range of 10-50 K/min.

As in the thermal degradation of OH-PLs, the remaining weight percents of COOH-PLs smoothly decreased to reach complete degradation regardless to the heating rates and end-groups concentration. By increasing the heating rate, the thermograms were shifted to higher temperatures. Increasing the heating rate from 10 to 50 K/min, the degradation temperature increased in the range of 60-70^{o}C at 50 percent weight loss. This increase in degradation temperature with increasing heating rate can be attributed to residence time of the sample at higher temperatures.

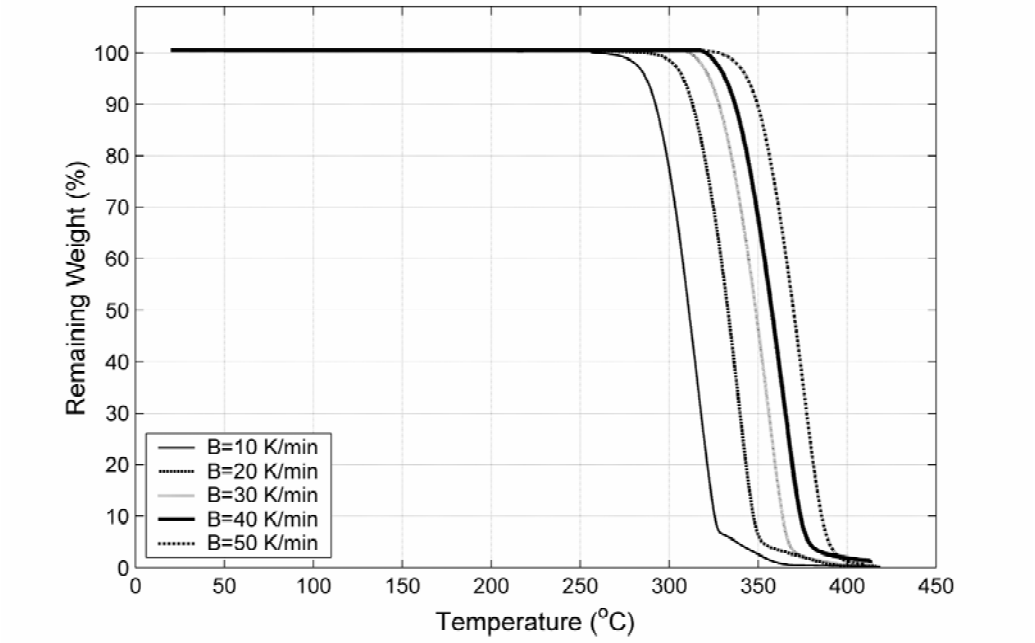

Figure 4.24: TGA Thermograms of 1-armed COOH-PL at heating rates of 10, 20, 30, 40, and 50 K/min.

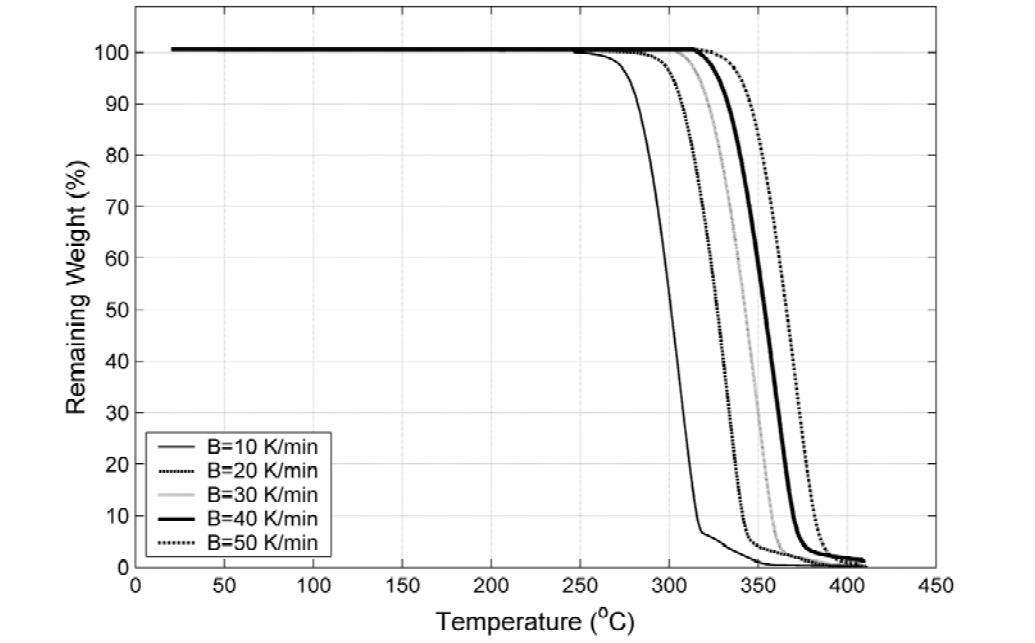

Figure 4.25: TGA Thermograms of 2-armed COOH-PL at heating rates of 10, 20, 30, 40, and 50 K/min.

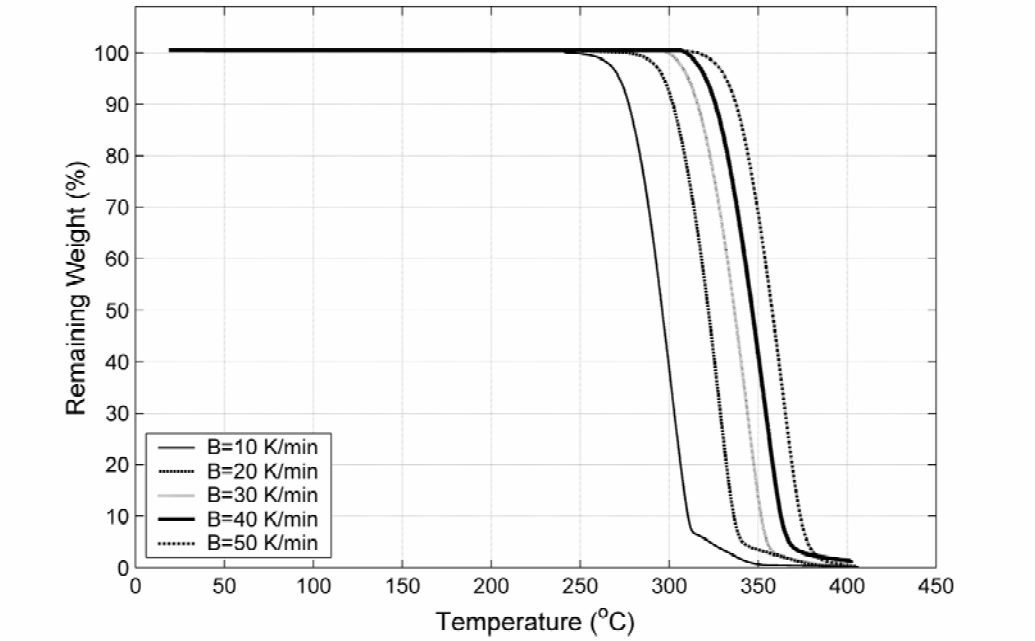

Figure 4.26: TGA Thermograms of 3-armed COOH-PL at heating rates of 10, 20, 30, 40, and 50 K/min.

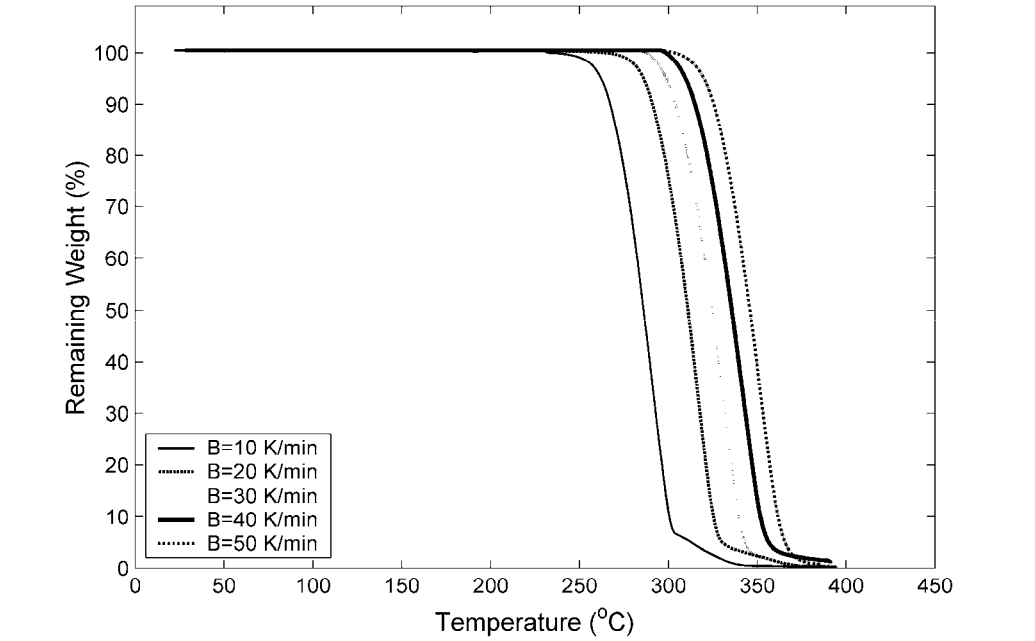

Figure 4.27: TGA Thermograms of 4-armed COOH-PL at heating rates of 10, 20, 30, 40, and 50 K/min.

The effect of end-group concentration on the thermal degradation behavior of COOH-PLs is depicted in Figure 4.28. Here, the thermograms of linear and multi-armed COOH-PLs obtained by heating the samples at a rate of 10 K/min. The thermal stability of COOH-PLs decreased with increasing end-group concentration. Again, as in the case of OH-PLs, the changes in degradation rate can be explained by the molecular weight of arms. Since the number average molecular weight of the polymers were about the same, the molecular weight of each arm decreased and the number of the thermal degradation sites increased as the number of end-groups on the polymer chain increased.

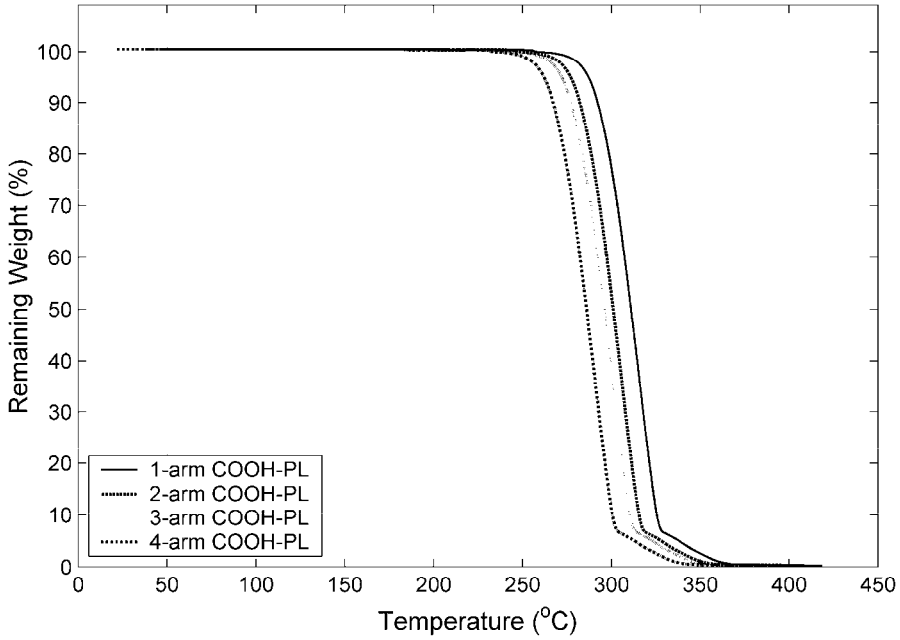

Figure 4.28: TGA Thermograms of 1-armed, 2-armed, 3-armed and 4-armed COOH-PLs at heating rate of 10 K/min.

To compare the thermal degradation behavior of OH and COOH functional PLs, the thermogravimetric data of linear PLs collected under the same conditions replotted together and depicted in Figure 4.29. As can be seen in this figure, the COOH functional PLs were thermally more stable than its OH functional counterpart. The difference was about 25°C at 50 percent degradation. The similar difference exists between 2-armed, 3-armed, and 4-armed OH and COOH functional PLs.

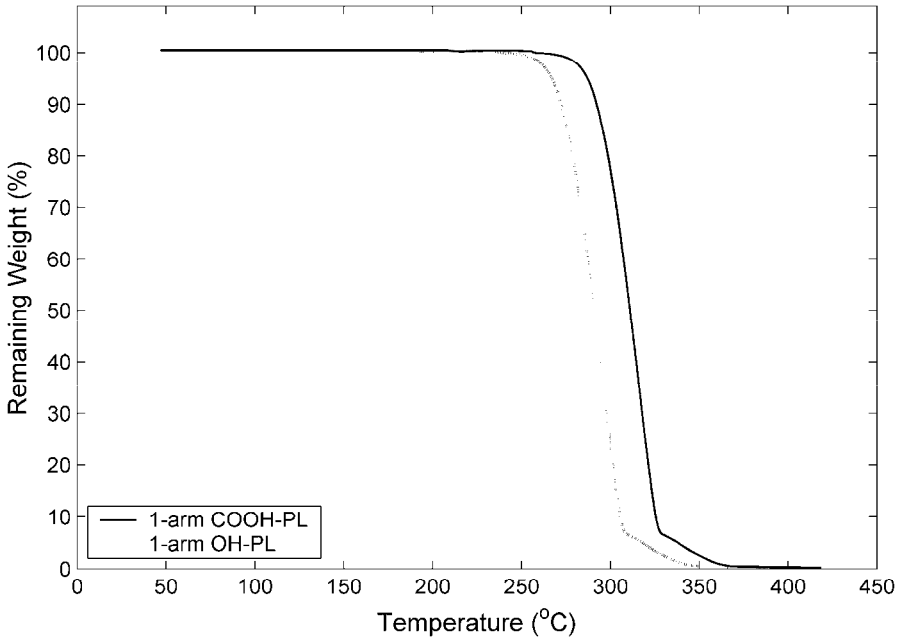

Figure 4.29: TGA Thermograms of 1-armed OH-PL and 1-armed COOH-PL at heating rate of 10 K/min.

The activation energies were also calculated using Ozawa's and Reich's approaches and the plots are depicted in Figure 4.30-4.37. In all these figures almost linear parallel lines were obtained using Ozawa's and Reich's equations and applying least squares method. The calculated activation energies at various fractions of thermal degradation of COOH-PLs are tabulated in Tables 4.15-4.18.

In both of the approaches, the calculated activation energies decreased slightly as the end-group concentration increased. The effect of end-group concentration on degradation rate can also be seen in Figure 4.28. The similar effects of end-group concentration were observed for OH-PLs and it can be related to the average molecular weight of the arms which decreased as the end-group numbers increased.

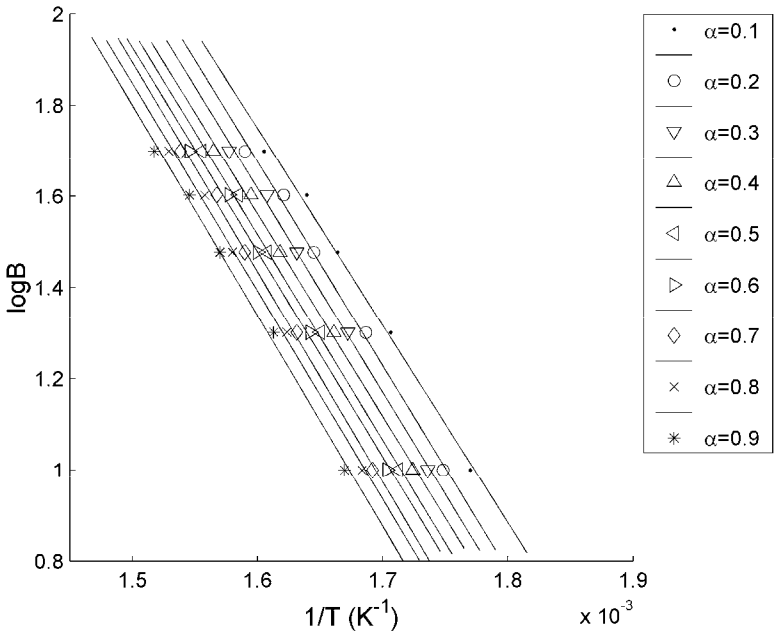

Figure 4.30: Ozawa plots of 1-armed COOH-PL at varied fractions of degradation, α = 0.9 to 0.1

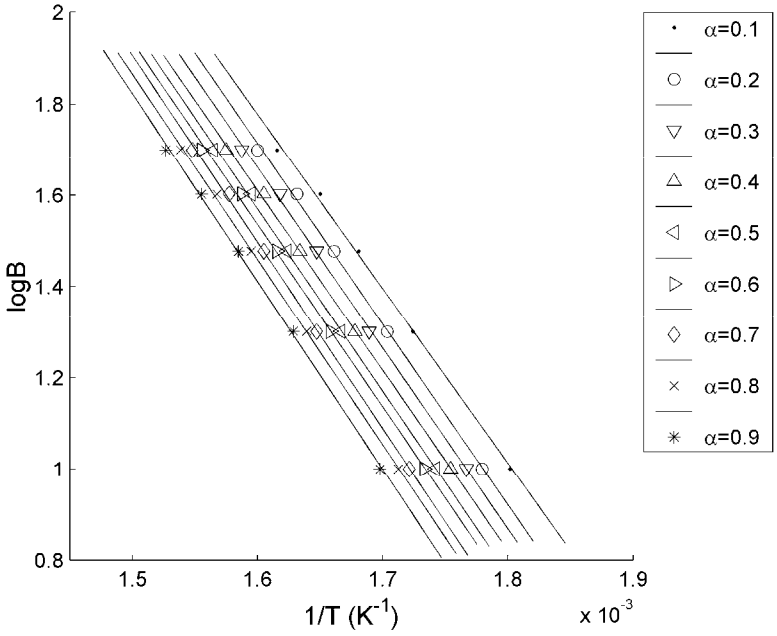

Figure 4.31: Ozawa plots of 2-armed COOH-PL at varied fractions of degradation, α = 0.9 to 0.1

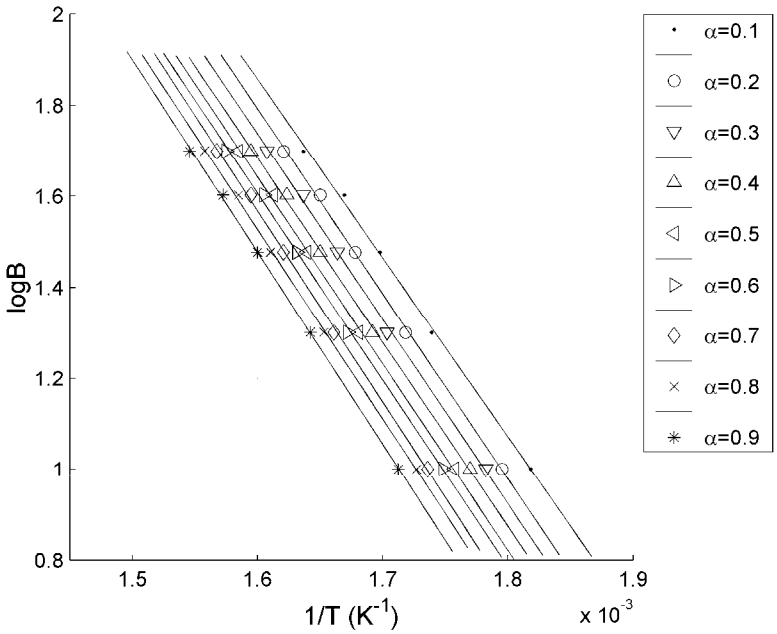

Figure 4.32: Ozawa plots of 3-armed COOH-PL at varied fractions of degradation, $\alpha = 0.9$ to 0.1

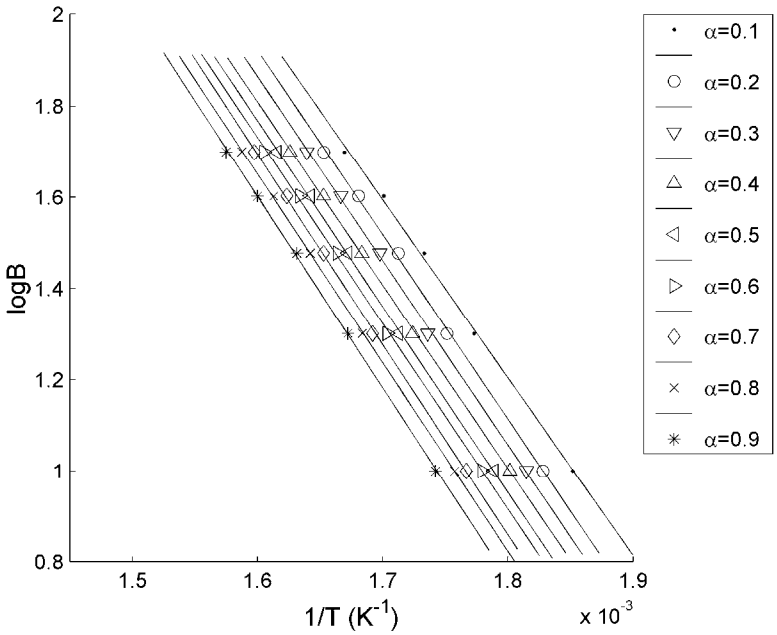

Figure 4.33: Ozawa plots of 4-armed COOH-PL at varied fractions of degradation, $\alpha = 0.9$ to 0.1

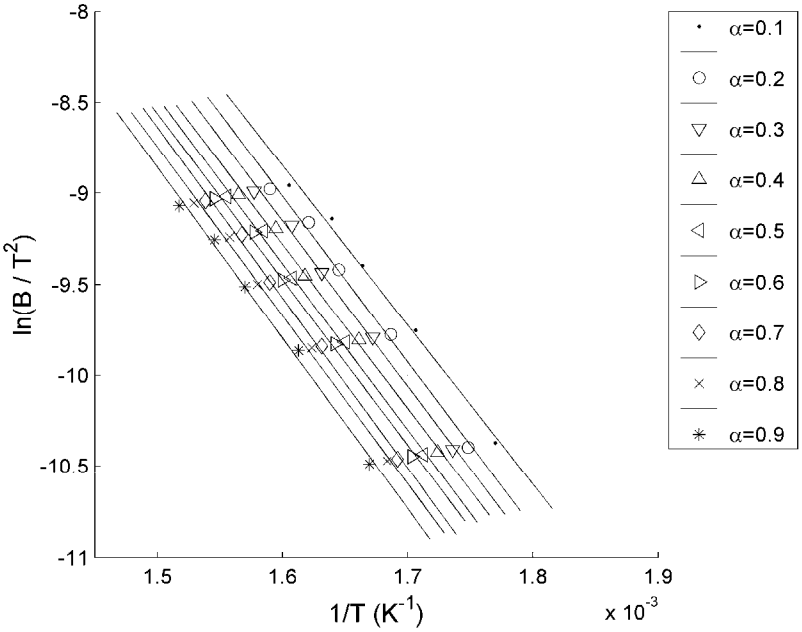

Figure 4.34: Reich plots of 1-armed COOH-PL at varied fractions of degradation, α = 0.9 to 0.1

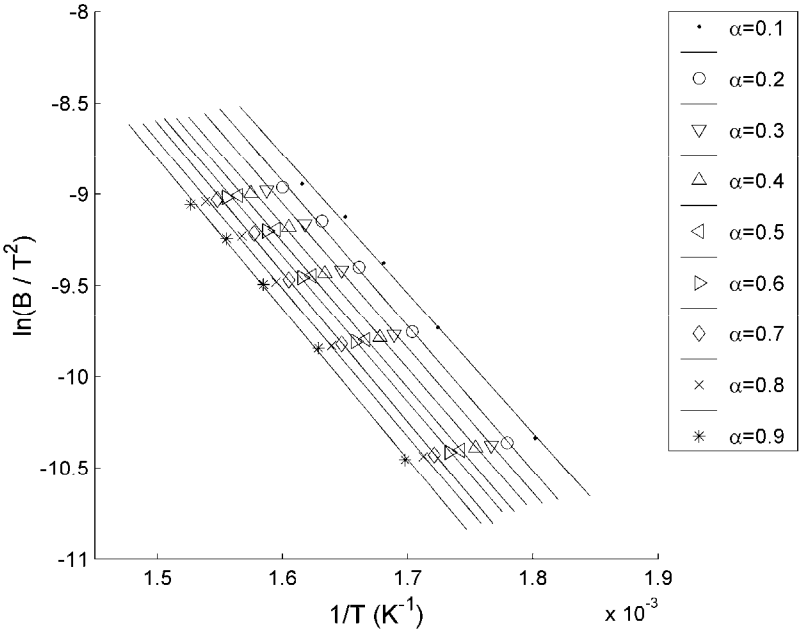

Figure 4.35: Reich plots of 2-armed COOH-PL at varied fractions of degradation, α = 0.9 to 0.1

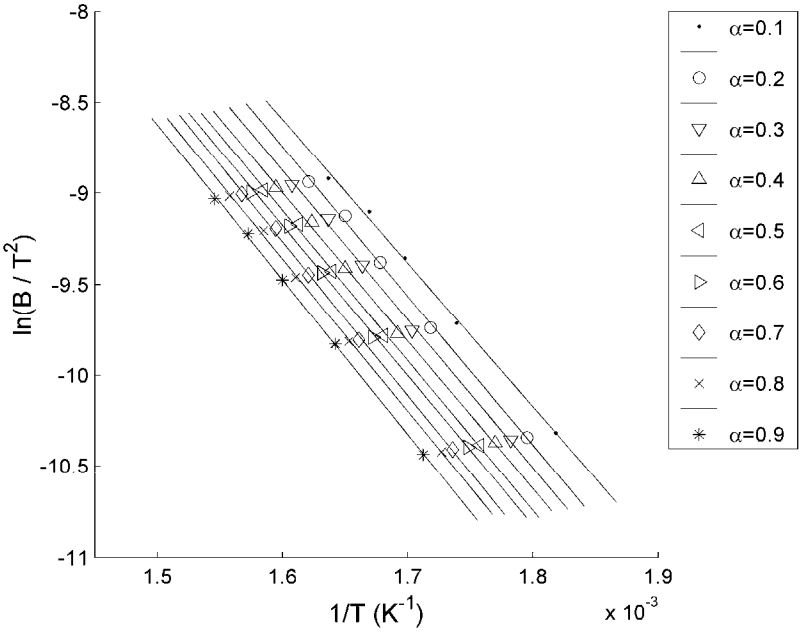

Figure 4.36: Reich plots of 3-armed COOH-PL at varied fractions of degradation, $\alpha = 0.9$ to 0.1

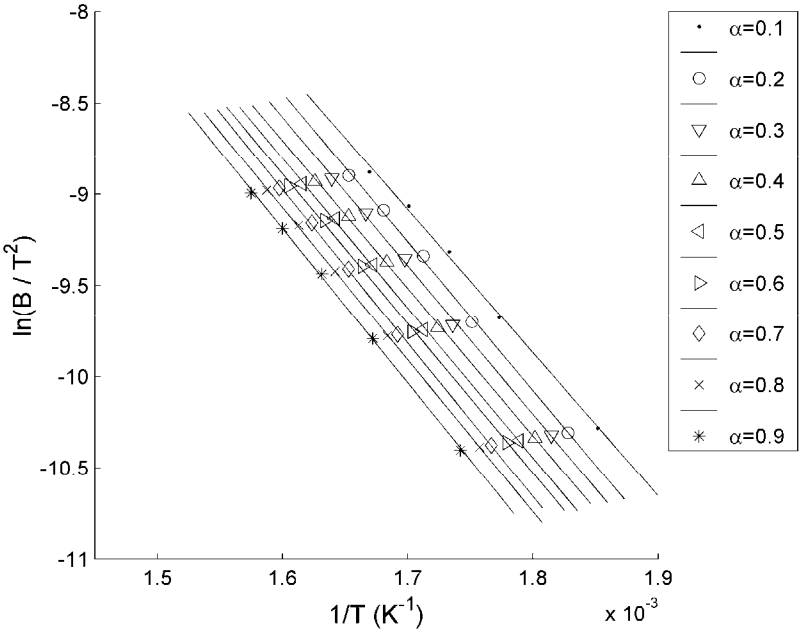

Figure 4.37: Reich plots of 4-armed COOH-PL at varied fractions of degradation, $\alpha = 0.9$ to 0.1

Table 4.15: Calculated activation energies using Ozawa and Reich approaches for 1-armed COOH-PL

B (^{o}C/min)	**10**	**20**	**30**	**40**	**50**		
α	**Temperature (^{o}C)**					**E_a Ozawa**	**E_a Reich**
0.1	292	313	328	337	350	78.5	72.8
0.2	299	320	335	344	356	81.4	75.7
0.3	303	325	340	349	361	81.3	75.5
0.4	307	329	345	354	366	80.8	74.9
0.5	311	333	349	358	370	81.9	76.0
0.6	314	336	352	361	374	81.7	75.8
0.7	318	340	356	365	377	83.8	77.8
0.8	321	343	360	369	381	82.9	76.9
0.9	326	347	364	374	386	84.0	77.9
Average E_a (kJ/mol)						81.8	75.9
Standard Deviation						±1.7	±1.6

Table 4.16: Calculated activation energies using Ozawa and Reich approaches for 2-armed COOH-PL

B (^{o}C/min)	**10**	**20**	**30**	**40**	**50**		
α	**Temperature (^{o}C)**					**E_a Ozawa**	**E_a Reich**
0.1	282	307	322	333	346	78.4	71.1
0.2	289	314	329	340	352	80.0	74.2
0.3	293	319	334	345	357	80.2	74.2
0.4	297	323	339	350	362	79.5	73.1
0.5	301	327	343	354	366	80.3	74.9
0.6	304	330	346	357	370	80.6	74.6
0.7	308	334	350	361	373	82.1	75.6
0.8	311	337	354	365	377	82.0	74.0
0.9	316	341	358	370	382	83.2	75.1
Average E_a (kJ/mol)						80.7	74.1
Standard Deviation						±1.5	±1.3

Table 4.17: Calculated activation energies using Ozawa and Reich approaches for 3-armed COOH-PL

B (^{o}C/min)	**10**	**20**	**30**	**40**	**50**		
α	**Temperature (^{o}C)**					**E_a Ozawa**	**E_a Reich**
0.1	277	302	316	326	338	70.9	70.4
0.2	284	309	323	333	344	79.4	73.6
0.3	288	314	328	338	349	79.7	73.8
0.4	292	318	333	343	354	79.0	72.4
0.5	296	322	337	347	358	79.6	73.1
0.6	299	325	340	350	362	79.5	73.7
0.7	303	329	344	354	365	80.0	75.1
0.8	306	332	348	358	369	81.4	73.2
0.9	311	336	352	363	374	82.5	74.0
Average E_a (kJ/mol)						79.1	73.3
Standard Deviation						±3.3	±1.3

Table 4.18: Calculated activation energies using Ozawa and Reich approaches for 4-armed COOH-PL

B (°C/min)	**10**	**20**	**30**	**40**	**50**		
α	**Temperature (°C)**					**E_a Ozawa**	**E_a Reich**
0.1	267	291	304	315	326	70.0	69.5
0.2	274	298	311	322	332	78.3	72.4
0.3	278	303	316	327	337	78.5	72.6
0.4	282	307	321	332	342	78.1	71.4
0.5	286	311	325	336	346	78.3	72.0
0.6	289	314	328	339	350	78.0	72.5
0.7	293	318	332	343	353	79.1	74.0
0.8	296	321	336	347	357	79.9	72.9
0.9	301	325	340	352	362	81.2	72.7
Average E_a (kJ/mol)						77.9	72.2
Standard Deviation						±3.2	±1.2

The calculated activation energies by Ozawa's and Reich's approaches increased slightly as the α increased from 0.1 to 0.9.

Similar to the thermal degradation of OH-PL, the calculated activation energies by Reich's approach are about 6 kJ/mol less than the calculated activation energies by Ozawa's approach. This difference may also be attributed to the assumptions during the derivation of the equations by these two approaches.

Table 4.19: Comparison of average E_a of OH-PLs with COOH-PLs

	Average E_a Ozawa	Average E_a Reich		Average E_a Ozawa	Average E_a Reich
1-armed OH-PL	76.5	70.7	1-armed COOH-PL	81.8	75.9
2-armed OH-PL	76.1	70.4	2-armed COOH-PL	80.7	74.1
3-armed OH-PL	75.5	70.0	3-armed COOH-PL	79.1	73.3
4-armed OH-PL	73.7	67.8	4-armed COOH-PL	77.9	72.2

The calculated average activation energies for the thermal degradation of OH-PLs and COOH-PLs are summarized in Table 4.19 for comparison. The increase in the activation energies by changing the OH groups to COOH could be because of the better stability of the PLs with COOH end-groups. The better thermal stability of COOH group

containing PLs was reported previously by others [11]. Probably, this is related with the OH at the chain terminal, which is more nucleophile than the acid group. Since OH is more nucleophile than COOH, it is easier to attack the polymer chain during the thermal degradation.

The activation energy for thermal degradation of high molecular weight (300,000 Da) linear poly(L-lactide) was reported as 113 kJ/mol by others [90]. The lower thermal stability (lower activation energy) of our polymers in comparison with that report can be related to the much lower molecular weight polymers contain fewer end-groups.

4.4. Crystallinity

In addition to the type and concentration of end-group, the crystal behavior is also an important factor for thermal degradation of PLs. The major factors for crystal behavior are crystal structure, crystallinity, and crystal size. Figure 4.38 shows the XRD patterns of linear and multi-armed OH-PLs. In these patterns, the PLs have the same crystal structure with different crystal sizes. The crystallinities are also expected to be different because of the average molecular weight of the arms on the polymer chain. In Figure 4.38, the decrease in intensities of peaks with increasing end-group concentration could be related to a decrease in degree of crystallinity.

The sizes of crystallities were calculated from full half maximum of peaks in XRD patterns of OH-PLs using the Peak Fit Computational Program and Scherer Equation:

$$d = \frac{0.9\lambda}{B\cos\theta} \tag{4.6}$$

where, λ is the wavelength of the source, 1.5408 nm, B is the full width half maximum and θ is the diffraction angle in radian.

The calculated crystalline domain sizes of linear and multi-armed OH-PLs are tabulated in Table 4.20.

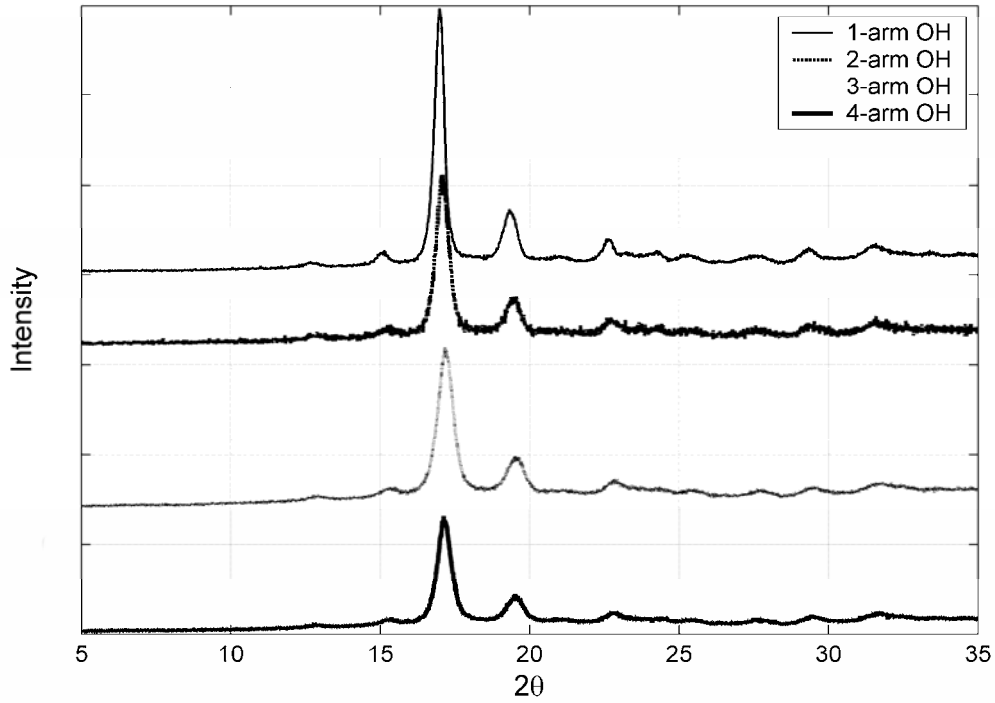

Figure 4.38: XRD Patterns of 1-armed, 2-armed, 3-armed and 4-armed OH-PL

Table 4.20: Crystallites Size of OH and COOH functional PLs.

	Crystallite Size (nm)		Crystallite Size (nm)
1-armed OH-PL	20.3	1-armed COOH-PL	17.5
2-armed OH-PL	15.9	2-armed COOH-PL	14.2
3-armed OH-PL	14.4	3-armed COOH-PL	13.6
4-armed OH-PL	13.7	4-armed COOH-PL	10.2

The calculated crystallite size of OH-PLs decreased with increased end-group concentration. There was about 7 nm decrease in size of crystalline domain from linear OH-PL to star-shaped OH-PL. This decrease could be explained by the decrease of molecular weight of each arm as the end-group concentration increased. Also, the increase in number of arms on each polymer molecule can decrease the amount of crsytallinity. It is

known that the linear polymers are more crystalline than branched polymers at a given molecular weight. The linear and multi-armed PLs show intense peaks at around 17^{o} and 19^{o}. These results are in good agreement with previous reports on linear and star-shaped PLs [12,91,92] and indicates that multi-armed OH-PLs have the same crystalline structure as the linear one.

The XRD patterns of linear and multi-armed COOH-PLs are shown in Figure 4.39. The calculated crystalline domain sizes using Scherer Equation are also tabulated in Table 4.20, and like OH-PLs, a decrease in crystallite sizes with increased end-group concentration was found. Comparing the crystallite sizes of OH-PLs and COOH-PLs, it can be seen that there is 1-3.5 nm decrese in COOH-PLs crystalline domains.

The peaks of COOH-PLs are at the same positions as OH-PLs, which indicates that changing the end-groups from OH to COOH did not affect the crystalline structure of the polymers.

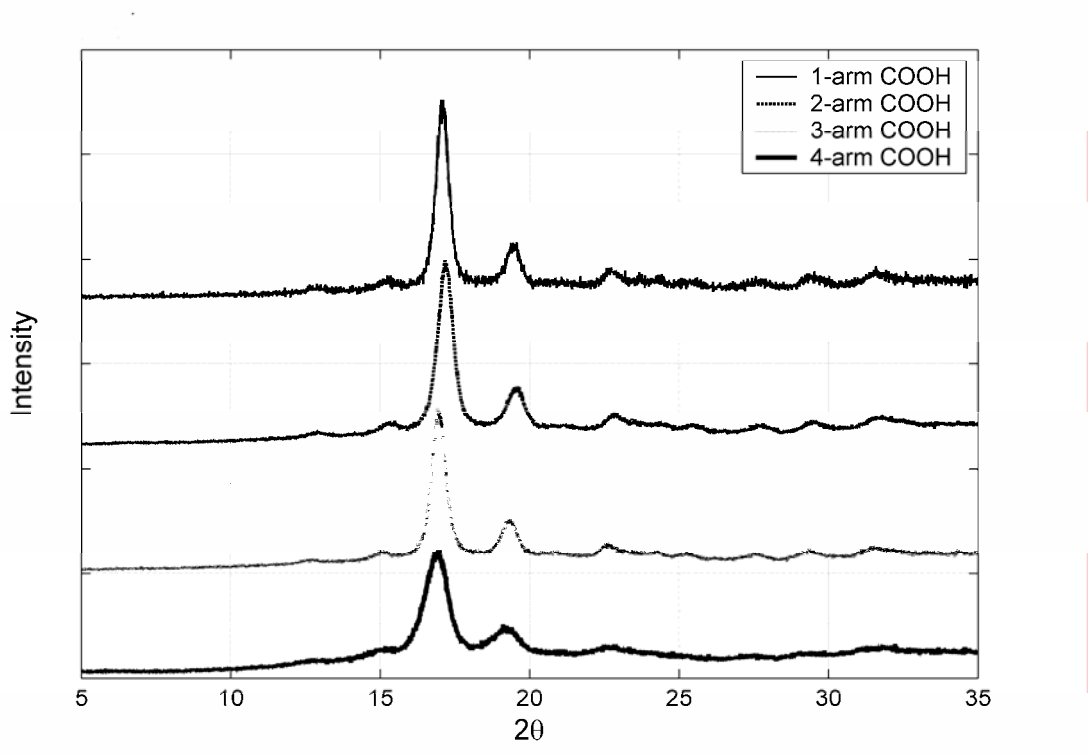

Figure 4.39: XRD Patterns of 1-armed, 2-armed, 3-armed, and 4-armed COOH-PL

CHAPTER 5

CONCLUSIONS

In this thesis, the synthesis, characterization, and thermal degradation of linear and multi-armed poly(L-lactide)s (PLs) are discussed in detail. Also, the effect of the type of the functional groups and their concentrations on crystallite size are discussed. The OH functional PLs were synthesized by ring opening polymerization of L-lactide using various alcohols as initiators and stannous dioctoate as a catalyst. The COOH functional PLs were prepared by reacting the OH-PLs with succinic anhydride. The resultant polymers were characterized by GPC and ^{1}H-NMR. The molecular weights determined by GPC and calculated from the peak intensities in ^{1}H-NMR spectra are found to be in good agreement.

The thermal degradation of the synthesized polymers was studied by TGA. The activation energies of the OH and COOH functional PLs were calculated from TGA thermograms at various degree of degradation applying Ozawa's and Reich's approaches. It was found that increasing the end-group concentration the thermal stability decreases. It was also found that COOH functional PLs are more stable than the OH functional PLs at the same end-group concentration.

The crystallinity of the OH and COOH functioanl PLs were investigated using X-Ray Diffractometer. The size of the crystalline domains were calculated using Scherrer Equation. It was found that there is a decrease in size with increasing end-group concentration in both OH and COOH functional PLs. Also, the acid modified PLs have smaller sizes than OH funtional counterparts. From the diffraction angles, it was concluded that the OH and COOH functional PLs are having the similar crystalline structures.

Further experiments should be carried out to synthesize higher molecular weight OH and COOH functional PLs in order to find out the effect of the end groups under polymer processing conditions. The effect of amine and non-functional end groups on the thermal stability of PLs should also be investigated. The crystallinity of the polymers

should be studied in detail on films using XRD and Differential Scanning Calorimeter (DSC) in order to find out the end-groups effect on the crystallization. Also, the hydrolytic degradation of these polymers should be investigated.

REFERENCES

[1] Vink, E. T. H.; Rabago, K. R.; Glassner, D. A.; Gruber, P. R. *Polym Degrad Stabil* 2003, 80, 403-19.

[2] Lunt, J. *Polym Degrad Stabil* 1998, 59, 145-152.

[3] Kricheldorf, H. R. *Chemosphere* 2001, 43, 49-54.

[4] Sodergard, A.; Stolt, M. *Prog Polym Sci* 2002, 27, 1123-63

[5] Jamshidi, K.; Hyon, S.-H.; Ikada, Y. *Polymer* 1988, 29, 2229-34.

[6] Grijpma, D. W.; Nijenhuis, A. J.; Pennings, A. J. *Polymer* 1990, 31, 2201-6.

[7] Grijpma, D. W.; Pennings A. J. *Macromol Chem Phys* 1994, 195, 1633-47.

[8] Dong, C-M.; Qiu, K-Y.; Gu, Z-W. *J Polym Sci Part A: Polym Chem* 2000, 38, 4179-84.

[9] Grijpma, D. W.; Zondervan G. J.; Pennings A. J.; *Polym Bull* 1991, 25, 327-33.

[10] Nakayama, A.; Kawasaki, N.; Arvanitoyannis, I.; Iyoda J.; Yamamoto N. *Polymer* 1995, 36, 1295-301.

[11] Lee, S-H.; Kim, S. H.; Han, Y-K.; Kim, Y. H. *J Polym Sci Part A: Polym Chem* 2001, 39, 973-985.

[12] Kim, E. S.; Kim, B. C.; Kim, S. H. *J Polym Sci Part B: Polym Phys* 2004, 42, 939-46.

[13] Amass, W.; Amass, A.; Tighe, B. *Polym Int* 1998, 47, 89-144.

[14] Hasirci, V. *Biodegradable Biomedical Polymers. Review of Degradation of and In Vivo Responses to Polylactides and Polyhydroxyalkanoates, in Biomaterials and Bioengineering Handbook,* ed. Wise, D. L., Marcel Dekker, Inc, NY, 2000, 141-55.

[15] Huffman, K. R.; Casey, D. J. *J Polym Sci Part A: Polym Chem* 1985, 23, 1939-54.

[16] Jong, S. J.; Arias E. R.; Rijkers D. T. S.; van Nostrum, C. F.; Kettenes-van den Bosch J.J.; Hennink W.E. *Polymer* 2001, 42, 2795-802.

[17] Cam, D.; Marrucci, M. *Polymer* 1997, 38, 1879-84.

[18] Tomihata, K.; Suzuki, M.; Sasaki, I. (Gunze Limited). U. S. Patent 6,616,687, 2003.

[19] Bhardwaj, R.; Blanchard, J. *Int J Pharm* 1998, 170, 109-17.

[20] Winet, H.; Bao, J. Y. *J Biomed Mater Res* 1998, 40, 567-76.

[21] Uhrich, K. E.; Cannizzaro, S. M.; Langer, R. S.; Shakesheff, K. M. *Chem Rev* 1999, 99, 3181-98.

[22] Kowalski, A.; Duda, A.; Penczek, S. *Macromolecules* 2000, 33, 689-95.

[23] Dubois, P.; Jacobs, C.; Jerome, R.; Tessie, P. *Macromolecules* 1991, 24, 2266-70.

[24] Kricheldorf, H. R.; Lee, S.; Bush, S. *Macromolecules* 1996, 29, 1375-81.

[25] Stevels, W. M.; Dijkstra, J. F. *Trends Polym Sci* 1997, 5, 300-5.

[26] O'Keef, B.; Monnier, S.; Hillmyer, M. A.; Tolman, W. B. *J Am Chem Soc* 2001, 123, 339-40.

[27] Eling, E.; Gogolewski, S.; Pennings, A. J. *Polymer* 1982, 23, 1587-93.

[28] Gogolewski, S.; Pennings, A. J. *J Appl Polym Sci* 1983, 28, 1045.

[29] Leenslag, J. W., Gogolewski, S.; Pennings, A. J. *J Appl Polym Sci* 1984, 29, 2829-42.

[30] Kricheldorf, H. R.; Kreiser-Saunder, I.; Boettcher, C. *Polymer* 1995, 36, 1253-59.

[31] Witzke, D. R.; Narayan, R.; Kolstad, J. J. *Macromolecules* 1997, 30, 7075-85.

[32] Nederberg, F.; Connor, E. F.; Moller, M.; Glauser, T.; Mock, A.; Nyce, G.; Hedrick, J. L. *Angew Chem Int Edit* 2001, 40, 2712-15.

[33] Myers, M.; Connor, E. F.; Glauser, T.; Mock, A.; Nyce, G.; Hedrick, J. L *J Polym Sci Part A: Polym Chem* 2002, 40, 844-51.

[34] Connor, E. F.; Nyce, G.; Myers, M.; Mock, A.; Hedrick, J. L. *J Am Chem Soc* 2002, 124, 914-5.

[35] Peter, J. A.; Veld, I.; Velner, E. M.; Van De Witte, P.; Hamhuis, J.; Dijkstra P. J.; Feijen, J. *J Polym Sci Part A: Polym Chem* 1997, 35, 219-26.

[36] Ryner, M.; Stridsberg, K.; Albertsson A-C.; von Schenck, H.; Svensson, M. *Macromolecules* 2001, 34, 3877-81.

[37] Kricheldorf, H. R.; Serra, A. *Polym Bull* 1985, 14, 497-502.

[38] Leenslag, J. W.; Pennings, A. J. *Makromol Chem* 1987, 188, 1809.

[39] Kricheldorf, H. R.; Sumbel, M. *Eur Polym J* 1989, 25, 585-91.

[40] Nijenhuis, A. J.; Grijpma, D. W.; Penning, A. J. *Macromolecules* 1992, 25, 6419-24.

[41] Kurcok, P.; Matuszowicz, A.; Jedlinski, Z.; Kricheldorf, H. R.; Dubois, P.; Jerome, R.; *Macromol Rapid Comm* 1995, 16, 513-19.

[42] Schwach, G.; Coudane, J.; Engel, R.; Vert, M. *Polym Bull* 1994, 32, 617-23.

[43] Engelberg, I.; Kohn, J. *Biomaterials* 1991, 12, 292.

[44] Vert, M.; Li, S. M.; Spenlehauer, G.; Guerin, P. *J Mater Sci Mater Med* 1992, 3, 432.

[45] Cooke, T. F. *J Polym Eng* 1990, 9, 171.

[46] Williams, D. F. *J Mater Sci* 1982, 17, 1233.

[47] Gilding, D.K.; Reed, A.M. *Polymer* 1979, 20, 1459.

[48] Cohn, D.; Younes, H.; Marom, G. *Polymer* 1987, 28, 2018.

[49] Gogolewski, S.; Mainil-Varlet, P. *Biomaterials* 1996, 17, 523-28.

[50] Sam, A.; Doherty, P.J.; Williams, D.F. *J Appl Polym Sci* 1994, 51, 1389-98.

[51] Ikada, Y.; Tsuji, H. *Macromol Rapid Comm* 2000, 21, 117-32.

[52] Schwach. G.; Vert, M. *Int J Biol Macromol* 1999, 25, 283-91.

[53] Pistner, H.; Bendix, D. R.; Muhling, J.; Reuther, J. *Biomaterials* 1993, 14, 291-8.

[54] Pistner, H.; Stallforth, H.; Gulwarld, R.; Muhling, J; Reuther, J.; Michel, C. *Biomaterials* 1994, 15, 439-50.

[55] Sodergard, A.; Pantke, M.; Selin, J-F. *Int Biodeterior Biodegrad* 1996, 38, 101-6.

[56] Hiltunen, K.; Seppala, J.V.; Itavara, M.; Harkonen, M. *J Environ Polym Degrad* 1997, 5, 167-73.

[57] Shirama, H.; Mizuma, K.; Umemato, K.; Yasuda H. *J Polym Sci Part A: Polym Chem* 2001, 39, 1374-81.

[58] Drumright, R.E.; Gruber, P. R.; Henton, D. E. *Adv Mater* 2000, 12, 1841-46.

[59] Karjomaa, S.; Suortti, T.; Lempiainen, R.; Selin, J-F.; Itavaara M. *Polym Degrad Stabil* 1998, 59, 333-6.

[60] Cai, H.; Dave, V.; Gross, R. A.; McCarthy, S. P. *J Polym Sci Part B: Polym Phys* 1996, 34, 2701-8.

[61] Hakkarainen, M.; Karrlsson, S.; Albertsson, A-C. *J Appl Polym Sci* 2000, 76, 228-39.

[62] Tsuji, H.; Miyauchi, S. *Biomacromolecules* 2001, 2, 597-604.

[63] Vert, M.; Li, S.; Garreau, H. *J Control Rel* 1991, 16, 15-26.

[64] Shih, C. *J Control Rel,* 1995, 34, 9-15.

[65] Tsuji, H.; Mizuno, A.; Yoshito, I. *J Appl Polym Sci* 2000, 77, 1452-64.

[66] Hakkarainen, M.; Albertsson, A-C.; Karlsson, S. *Polym Degrad Stabil* 1996, 52, 283-91.

[67] Joziasse, C. A. P; Grijpma, D.W; Bergsma, J. E.; Cordewener, F.W; Bos, R.R. M; Pennings, A. J. *Colloid Polym Sci* 1998, 276, 968-75.

[68] Li, S.; McCarthy, S. *Biomaterials* 1999, 20, 35-44.

[69] Chu, C.C. *Polymer* 1985, 26, 591-4.

[70] Hiljanen-Vainio, M. P.; Orava P.A.; Seppala, J.V. *J Biomed Mater Res* 1997, 34, 39-46.

[71] Hiltunen, K.; Tuominen, J.; Seppala, J.V. *Polym Int* 1998, 47, 186-92.

[72] Li, S.M.; Garreau, H.; Vert, M. *J Mater Sci Mater Med* 1990, 1, 123-30.

[73] Cha, Y.; Pitt, C.G. *Biomaterials* 1990, 11, 108-12.

[74] Sodergand, A.; Selin, J-F.; Nasman, J. H. *Polym Degrad Stabil* 1996, 51, 351-59.

[75] Cooper, D. R.; Sutton, G. J.; Tighe B.J *J Polym Sci Part A: Polym Chem* 1973, 11, 2045-56.

[76] Kopinke, F-D.; Remmler, M.; Mackenzie, K. *Polym Degrad Stabil* 1996, 52, 25-38.

[77] Gupta, M.C.; Deshmukh, V. G. *Colloid Polym Sci* 1982, 260, 308-11.

[78] van Oepen, R.; Michaeli W. *Clin Mater* 1992, 10, 21-8.

[79] Zhang, X.; Wyss, U.P. *Polym Bull* 1992, 27, 623-9.

[80] Tighe B.J. *Dev Polym Degr* 1984, 5, 31-77.

[81] McNeill, I. C.; Leiper, H. A. *Polym Degrad Stabil* 1985, 11, 309-26.

[82] Kotliar, A. M. *J Polym Sci Macromol Rev* 1981, 16, 367-95.

[83] Porter, R. S.; Wang, L. H. *Polymer* 1992, 33, 2019-30.

[84] Doyle, C.D. *J App Polym Sci* 1961, 5, 285-92.

[85] Reich, L. *Polymer Letters* 1964, 2, 621.

[86] Ozawa, T. *Bull Chem Soc Japan* 1965, 38, 1881-6.

[87] Reich, L *Polymer Letters* 1965, 3, 231-4.

[88] Coats, A. W.; Redfern, J. P. *Polymer Letters* 1965, 3, 917-20.

[89] Friedman, H. L. *J Polym Sci Part C*,1965, 6, 183.

[90] Grijpma, D. W. *High Impact Strength Poly(Lactide)- Tough Biodegradable Materials, PhD Thesis,* University of Groningen, The Netherlands, 1993.

[91] Cho, J. D.; Baratian, S.; Kim, J.; Yeh, F.; Hsiao, B. S.; Runt, J. *Polymer* 2003, 44, 711-7.

[92] Ikada, Y.; Jamshidi, K.; Tsuji, H.; Hyon, S. H.; *Macromolecules* 1987, 20, 904.